Experimental Investigation and Optimization of Delamination Factors in the Drilling of Jute Fiber Reinforced Polymer Biocomposites with Multiple Estimators

Bachir Adda
Universite du 20 aout 1955 de Skikda
Ahmed Belaadi (ahmedbelaadi1@yahoo.fr)
Universite du 20 aout 1955 de Skikda
Messaouda Boumaaza
Université 8 Mai 1945 Guelma
Mostefa Bourchak
King Abdulaziz University

Research Article

Keywords: Drilling/Machining, Composite delamination, Statistical properties/methods, RSM/ANN, Genetic algorithm optimization

Posted Date: May 18th, 2021

DOI: https://doi.org/10.21203/rs.3.rs-519941/v1

Version of Record: A version of this preprint was published at The International Journal of Advanced Manufacturing Technology on July 13th, 2021. See the published version at https://doi.org/10.1007/s00170-021-07628-9.

Experimental Investigation and Optimization of Delamination Factors in the Drilling of Jute Fiber Reinforced Polymer Biocomposites with Multiple Estimators

Bachir Adda[1,2], Ahmed Belaadi [1,3*], Messaouda Boumaaza[3], Mostefa Bourchak [4]

[1]Département de Génie Mécanique, Faculté de Technologie, Université 20 Août 1955- Skikda, Algérie.
[2] Laboratoire LGMM, Université 20 Août 1955- Skikda, Algérie.
[3] Laboratoire LSPN, Université 8 mai 1945 Guelma, Algérie.
[3] Laboratoire de Génie Civil & Hydraulique (LGCH), Université 8 Mai 1945 Guelma, Algérie.
[4] Aeronautical Engineering Department, King Abdulaziz University, Jeddah, Saudi Arabia.

*Corresponding author, Dr, A Belaadi (http://orcid,org/0000-0002-6059-3974)

E-mail addresses: a,belaadi@univ-skikda,dz , ahmedbelaadi1@yahoo,fr

Abstract

Currently, the manufacture of composite structures often requires material removal operations using a cutting tool. Indeed, since biocomposites are generally materials that do not conduct electricity, electro-erosion cannot be utilized. As a result, the processes that can be used are limited to conventional machining, called chip removal machining, such as drilling. Delamination factors are widely recognized for controlling the damaged area (delamination) induced by drilling in industry. As discussed in the literature, several approaches are available to evaluate and quantify the delamination surrounding a hole. In this context, the objective of this study is to compare the three F_d evaluation methods that have been most frequently used in previous investigations. To this end, three rotational and feed speeds and three BSD tool diameters were selected (L_{27}) for drilling 155 g/m^2 density jute fabric reinforced polyester biocomposites. The response surface methodology (RSM) and artificial neural networks (ANNs) were applied to validate the results obtained experimentally as well as to predict the behavior of the structure depending on the cutting conditions.

Keywords: Drilling/Machining; Composite delamination; Statistical properties/methods; RSM/ANN; Genetic algorithm optimization.

1. Introduction

Natural fibers are initially biodegradable and are often considered neutral with respect to CO_2 emissions into the atmosphere because their biodegradation only produces a certain amount of carbon dioxide[1]. Biocomposites are therefore easier to recycle. Moreover, if their matrix is biodegradable, these materials are also compostable after grinding when the material is too degraded [2]. Biocomposites are mainly used in several fields, such as construction, sports, and transport [3, 4]. On the other hand, the manufacturing processes and implementations of these biomaterials are poorly controlled because of the natural origin of the biofibers. Indeed, to better understand the behavior of biocomposites, in-depth scientific studies have been conducted by several researchers [5, 6]. Currently, a wide variety of plant fibers are currently used as reinforcements for different matrices [7, 8], such as sisal.[9], jute [10], *Agave americana L.* [11], flax [4, 12–14], *Washingtonia filifera* [15], date palm [16, 17] and pineapple [18].

To date, in several studies, the machining process has been investigated during the drilling of glass, aramid and carbon composites to study the interaction mechanisms between the cutting tools and the material and to determine the most influential machining parameters with respect to the behavior of the fibers; thus, the most suitable process can be chosen [19–27]. On the other hand, there have been only a limited number of studies in the literature that address the machining of biocomposites [28–54] as well as comparative studies between biocomposites and glass fiber composites [55]. However, the milling process [56, 57] and orthogonal cutting [58, 59] have been much less studied.

Chandramohan and Rajesh [60] showed that the drill geometry has an effect on the drilling torque. These researchers relied on the drilling torque results of two types of drills for the prediction of the drilling torque when machining biocomposites. Indeed, the drilling torque with a multisided drill was greater than that with a twist drill at a low cutting speed. The effect of the drill geometry on the drilling quality of laminated composites has been the subject of much research. In investigations on the drilling of FFRPs using drills of different geometries, Rezghi Maleki et al. [61] found that due to the difference in the cutting mechanism, the type of drill used had a great influence on the pushing force and thereby on the delamination size. Furthermore, their ANOVA showed that the choice of drill bit had a great impact on the delamination factor (67.27%) and surface roughness (74.44%). However, the tool geometry has been shown to have less impact on the residual tensile strength of FFRP composites [62].

Bajpai and Singh [30] experimentally investigated the drilling behavior of the natural fiber reinforced biodegradable biocomposite sisal/PP. In this study, the effect of cutting parameters

(spindle speed, feed speed and tool geometry) and drill geometry (twist drill and tool trepanation) was investigated. The investigation, using ANOVA, showed that the influence of the tool geometry is more important than other parameters. In other work presented by Bajpai et al. [31], the drilling performance of the biodegradable biocomposite sisal and Grewia optiva reinforced polylactic acid was studied using tool geometries, namely, twist, Jo, and parabolic drills with 8 mm diameter solid carbide. The RSM method was used to optimize the cutting parameters in terms of the drilling thrust force and torque and drilling-induced damage. This study showed that the geometry of the tools is an important factor influencing the forces and damage induced by drilling. Davim and Reis [63] experimentally studied the influence of the tool material and geometry, such as a straight shank drill bit and Brad & Spur drill. Their work focused on producing less entry and exit delamination on carbon reinforced epoxy composite laminates. Chaudhary and Gohil [35] conducted an experimental study of the drilling performance, e.g., the thrust force, torque and exit delamination factor, on polyester/bidirectional cotton fiber biocomposites by varying the cutting parameters, namely, the spindle speed and feed speed geometry of a 10 mm diameter drill. In addition, the tests were carried out by the Taguchi orthogonal method (L_{27}) to optimize the cutting forces and damage using a one-way analysis (ANOVA) method. A comparative study developed by Athijayamani et al. [55] between two composite materials (epoxy/glass and epoxy/sisal) was conducted to analyze the effect of the two different tungsten carbide drill tool geometries (6 mm in diameter). The machining operation was realized with a classical helical drill and a Brad type (BSD) tool. In addition, the experiments were carried out at a constant spindle speed of 2800 rev/min with two feed rates (0.05 and 0.2 mm/rev). Venkateshwaran and ElayaPerumal [36] investigated the influence of drilling conditions (spindle speed and feed speed) using a constant 10 mm diameter HSS drill on the exit delamination factor damage of an epoxy matrix reinforced short banana fiber green biocomposite. The damage was analyzed using the ultrasonic C-scan technique. Moreover, the obtained results were evaluated using ANOVA. Ismail et al [39] studied the drilling behavior of different drill tool diameters on biodegradable composite laminates made of natural hemp fibers by varying the spindle speed and feed speed. The Taguchi method according to the L_{16} orthogonal network method was chosen. These authors concluded that the optimal results for delamination and surface roughness were obtained at a lower cutting speed and feed speed. In a similar work, Abilash and Sivapragash [41] studied the effect of experimental drilling parameters using the Taguchi method (L_{18} orthogonal network). In this work, the force output, torque and delamination were studied by drilling holes in green biodegradable composite polyester laminates reinforced with natural fibers treated with bamboo. ANOVA was adopted

to determine which drilling parameters were statistically significant. Athijayamani et al. [37] studied the drilling behavior of polyester-reinforced sisal and roselle fiber hybrid green composites. The fibers were treated using an alkali treatment of 10% NaOH for different durations. A constant dill (8 mm HSS) was used to perform the drilling process. The obtained results suggest that a better dimensional stability was reached by using a 30% by weight of fiber treatment for 8 h. Recently, Lotfi et al. [14] examined the drilling performance of a developed high-strength NFRC laminate (flax/PLA) and evaluated the influence of the cutting parameters, feed rate and spindle speed using two drills (HSS twist drill and carbide drill) on the generation of the minimum drilling force and drilling-induced damage. The authors concluded that the lowest damage with a good quality of the hole of the flax/PLA biocomposite is achieved with the HSS twist drill, a spindle speed of 2550 rpm and a feed rate of 0.08 mm/rev. In addition, this drill demonstrated better hole quality than carbide drills and results in a nearly 60% lower thrust force. In other recent work, Parthipan et al. [64] conducted interesting research that focused on the effect of the drilling performance of silane-treated silicon (IV) oxide particles dispersed in an epoxy matrix reinforced with kenaf fibers. The drilling behavior of the biocomposite showed that the addition of nano-silicon(IV) oxide and silane-treated kenaf fiber maintains high dimensional stability, lower friction penetration, a lower thermal affected zone and lower tool wear. Recently, Belaadi et al. [28] performed interesting research on the effect of drilling parameters such as the spindle speed, feed rate and drilling diameters on jute/polyester staple fiber biocomposites to estimate the influence of the delamination factor Fd. In other recent work by Belaadi et al. [46], an artificial neural network (ANN) model was developed to evaluate the direct and interaction effects of cutting parameters to analyze delamination. In their experiments, epoxy matrix jute fabric sheets were drilled three times for each cutting condition, and the hole exit damage was measured using a high-resolution scanner. The resulting image was subsequently processed by ImageJ to calculate the delamination factor. The results revealed that delamination is sensitive to each cutting parameter and that a combination of a high cutting speed and a low feed rate can minimize it. Furthermore, the regression analysis established a very good match between the predicted and experimental values of the delamination factor. This model establishes a nonlinear relationship between the drilling parameters and the delamination factor.

Indeed, most of the damage induced by the drill during the drilling process is located in the internal or external region of the biocomposite, where the evaluation of the latter is a difficult task. To quantify the size, shape and region of the delamination area, it is essential to use

microstructural analysis supported by image processing software. The visual inspection technique creates special problems for quantifying the delamination of biocomposites. From the literature review, it can be stated that few research studies have discussed the area of drilling of natural fiber biocomposites. In other words, there is still an important field of research in the field of machining biocomposites. In this context, this study focuses on the effect of drilling machining parameters on the delamination factor (*Fd*) of woven jute fabric/polyester (WJFP)-reinforced epoxy biocomposites. For comparison, different expressions for the evaluation of the delamination damage factor in drilling were used. A tool with different diameters was chosen, such as a wood drill (Brad & Spur), to estimate the influence and the simultaneous interaction of the input parameters on the *Fd* factor. Additionally, the response surface methodology (RSM) and artificial neural networks (ANNs) were used for *Fd* evaluation to estimate the influence and interaction of the cutting parameters at the exit of the drilling delamination. Finally, optimization functions such as the desirability based on the RSM, genetic algorithm (GA) and function (fmincon) were used to confirm the optimal combination of optimal cutting parameters (*f*, *N* and *d*) for the biosandwich structures studied in this work.

2. Materials and methods

2.1. Biocomposites manufacturing

In the present study, the reinforcement consisted of bidirectional jute fibers (**Figure 1**) with a basis weight of 155 g/m^2 (28 × 23 threads/100 mm) and polyester resin with a density of 1.410 kg/m^3. The polyester resin and jute fabric were supplied locally. The average mechanical characteristics of the polyester resin, namely, a 32 MPa tensile strength, a 2.7% elongation and a Young's modulus equal to 1.12 GPa, were described by Belaadi et al. **[28]** . The biocomposite samples (jute/polyester) were developed using the contact molding and hand lay-up process; the fabric was previously fabricated and then cut to dimensions of 280 × 280 mm. The obtained biocomposite samples were rectangular sheets, which were 280 mm in length, 280 mm in width and approximately 5.5±0.2 mm in thickness, consisting of five layers. Furthermore, the fiber content of the biocomposite laminates was 30 wt%. The processing of the polyester resin was carried out by catalysis and polymerization in proportions of approximately 1 to 1.5% by mass. The mixture (fiber/matrix) was cured and kept in the mold for 24 hours under standard atmospheric pressure (1 bar) and at an ambient temperature of 26°C until the end of the polymerization. To allow the mixture to polymerize, the plates were kept in open air for 15 days to ensure complete polymerization of the resin. The samples were finally postcured at a temperature of 60°C in an oven for 5 hours. The specimens for the drilling experiments were

cut to the following dimensions, namely, 260 × 90 × 5.5 mm^3, using a diamond saw with water lubrication to avoid excessive heating during cutting. Subsequently, the specimens were air-dried at room temperature (23°C) for 20 days.

2.2. Drilling experimental procedure

The drilling tests were performed using a MOMAC universal milling machine equipped with a 1400 rpm spindle with a feed rate of 4.6 to 1040 mm/rev [28, 46], and all drilling was performed on this machine. During the drilling phase, to limit the bending of the parts to avoid amplifying the defects at the exit of the hole, a solid steel support was placed under the composite parts. To carry out the drilling tests, the geometry of the workpiece was 260 × 90 × 5.5 mm^3, and **Figure 1** shows a workpiece fixation system. In this study, Brad & Spur drills with different diameters (5 mm, 7 mm and 10 mm) were used, and the shape and geometry of the tool are shown in **Figure 1**. The drilling of the holes in this study was performed in a single phase. To ensure a well-sized hole and prevent the wear of the drilling tool, the drill bit was renewed every four to five operations. The drilling operations were performed dry, without coolant. The spindle speeds were 355, 710 and 1400 rpm, and three feed rates were chosen (50, 108 and 190 mm/min). The cutting parameters were selected following a literature review presented in **Table 1**.

Then, the drilled specimens were scanned using a high-resolution scanner up to 2400 × 4800 dpi (48-bit internal color depth) to obtain a high-precision image. The resulting digital images were then imported and processed in *ImageJ* (free software v1.47, published by the National Institute of Health, USA [50, 51, 65]) to evaluate the damage area of the drilled hole *Fd.* The threshold filter was adjusted to highlight the delamination surrounding the hole. Delamination represents one of the major damage defects in drilled laminate composites. **Figure 2** shows the processing procedure adopted to determine the different damage areas of the hole. The three calculation methods used for the determination of F_d in this study under different machining conditions are presented in **Table 2**.

2.3. Experimental design

Table 3 shows the values of the response parameters Fd_1, Fd_2 and Fd_3 determined under different experimental configurations. The experimental design of this study was an orthogonal (*L27*) central composite design (*CCD*) array. This design was adopted to limit the number of experiments, and thus, the experimental expense and time was reduced. Three groups of levels,

namely, the drill diameter (*d*), spindle speed (*N*), and feed rate (*f*), and three levels in each group were considered (**Table 4**).

3. Results and discussion

3.1 Influence of the drilling parameters on the delamination factor

The condition of the drilled holes at the exit and entrance (#3, #12 and #21) with feed rates of 50, 108, and 190 mm/min and a spindle speed of 355 rpm was examined (**Figure 2a** and **b**). The machined jute/polyester fiber composites were digitally imaged with a standard scanner with a resolution of 4800 pixels. Image processing software was used to create two concentric circles. The damage caused by drilling the holes in the composite is related to the delamination factor. The choice of cutting parameters and the fiber fabric used during the design process is a fundamental concern for delamination. Indeed, the determination of the delamination factor *Fd* of biosandwich structures using Brad & Spur drills (BSD) is related to many factors, such as the feed rate, cutting speed and tool diameter. Additionally, it is appropriate to determine the different parameters for the calculation of the delamination factors performed on the drills and to analyze the image obtained through this calculation (**Figure 2c**).

3.3 Response surface methodology and ANOVA for delamination factor

The response surface analysis method was used to process the experimental results to find the correlation that exists between delamination and the different parameters of the composite. Indeed, the response surface methodology (RSM) is a mathematical and statistical approach that is generally used in engineering sciences and cutting operations [66]. Moreover, this method is based on an empirical modeling approach that aims to find the relationship between input and output parameters, such as the delamination *Fd*, by changing the different cutting parameters when drilling the biosandwiches. The mathematical equations of the regression are reported in **Table 5** for the different delamination factors obtained by Design-Expert software, which recommended the quadratic models. These models are second-order mathematical models based on the RSM. **Figure 3** shows the relationship between the probability of the residuals and the predicted and experimental values of the delamination *Fd* for Fd_1, Fd_2 and Fd_3. For the *Fd* delamination residuals, the normal probability curve shown in **Figures 3a** and **b** indicates that the residuals form a straight line, implying that the errors are correctly distributed. These results demonstrate that the fit of the model is excellent. Thus, the results obtained show satisfactory agreement of the regression model since the predicted values are

statistically identical to the experimental values with a 95% confidence level. The significance synthesis of the results revealed that the quadratic model is statistically significant for the delamination analysis. In **Table 6**, the results of the ANOVA quadratic model for Fd_1, Fd_2 and Fd_3 are presented; however, the model terms *f*, *d*, $N \times d$, N^2, and d^2 are significant, while *N* and $f \times N$ are also significant for BSD only. The R^2 coefficient and adjusted R^2 coefficient corresponding to delamination are 95.07% and 95.47% for Fd_1, 89.21% and 83.49% for Fd_2, and 96.65% and 93.35% for Fd_3, respectively. Thus, it is clear that this regression model provides a perfect fit between the responses and the independent factors. In this study, to confirm the effect of the cutting-related parameters on the responses, the statistical tools called "p-value" and "F-value" (the ratio of the mean square to the mean square and the ratio of the mean square to the mean square of the experimental error, respectively) are described. If the p-values are less than 0.05 (p-value < 0.05), then the conditions required by the model are significant. The present analysis is performed at a 5% significance level, i.e., for a 95% confidence level. According to ANOVA, the models were highly statistically significant ($p < 0.0001$). In addition, the F-values for Fd_1, Fd_2 and Fd_3 are 36.46, 15.61 and 41.58, respectively. Due to the larger F-value, it appears that the diameter d and feed rate f are the most significant parameters for the delamination of composites Fd_1, Fd_2 and Fd_3 compared to cutting speed N. However, for Fd_1, the model terms *f*, *d*, $f \times d$, $N \times d$, $f \times f$ and $d \times d$ are significant, while only the terms *f* and d are significant for Fd_2, and *f*, *N*, *d* and $N \times d$ influence Fd_3. The most important variable influencing the response value of the delamination factors is the drill diameter. Then, the second variable influencing the response value is the feed rate. Therefore, it appears that the diameter of the drill is the main parameter that affects the delamination factor, followed by the feed rate and the cutting speed. In addition, the contribution of the d-factor is most significant for Fd_1, Fd_2 and Fd_3. The diameter of the drill was more significant with respect to delamination than the feed rate and cutting the speed.

3.3 2D surface plots for the delamination factor

The results in **Figure 4** provide a mapping of the response surfaces obtained for delamination at the exit of composites machined by BSD drills as a function of the feed rate (*f*), cutting speed (*N*) and diameter (*d*). For a constant diameter, the delamination does not exceed 1.10 for the factor Fd_1 with *f* between 50 and 58 mm/min and *N* from 1241 to 1400 rev/min, but it exceeds 1.5 when *f* is between 123 and 190 mm/min and *N* from 355 to 773 rev/min (**Figure 4a**). For tool Fd_2, notably, the delamination does not exceed 1.2 when *f* is between 50 and 57 mm/min and *N* is between 459 and 992 rev/min, while it exceeds 2.0 when *f* is between 185 and 190

mm/min and *N* is between 355 and 658 rev/min (**Figure 4b**). For tool Fd_3, we also note that the delamination does not exceed 1.1 for *f* between 50 and 78 mm/min and *N* from 355 to 1400 rev/min, but it exceeds 1.3 when *f* is between 164 and 190 mm/min and *N* from 355 to 1400 rev/min (**Figure 4c**). **Figures 4d-f** show for a constant cutting speed how the feed rate and drill diameter significantly affect delamination Fd_1, Fd_2 and Fd_3 using the BSD drills. Delamination is less than 1.2 for Fd_1 when *f* is between 50 and 88 mm/min and *d* is between 5 and 5.4 mm, less than 1.5 for Fd_2 when *f* is between 50 and 58 mm/min and *d* is between 5 and 5.2 mm, and less than 1.2 for Fd_3 when *f* is between 50 and 126 mm/min and *d* is between 5 and 6.5 mm. It also appears that the delamination is greater than 1.8 for Fd_1 when *f* is between 50 and 190 mm/min and *d* is between 6.6 and 10 mm, greater than 3 for Fd_2 when *f* is between 90 and 190 mm/min and *d* is between 9.8 and 10 mm, and greater than 1.8 for Fd_3 when *f* is between 112 and 190 mm/min and *d* is between 8.5 and 10 mm. The effect of drill tool diameter and cutting speed on delamination at a constant feed rate is shown in **Figures 4g-h**. The delamination is less than 1.2, 1.5 and 1.1 for Fd_1, Fd_2 and Fd_3, respectively, when *d* and *N* are between 5-5.2 mm and 721-1400 rev/min for Fd_1, 5-6.4 mm and 355-1400 rev/min for Fd_2 and 5-5.7 mm and 355-1400 rev/min for Fd_3. Furthermore, it is also observed that the *Fd* value exceeds 1.8, 2.5 and 1.6 when *d* and *N* are between 7.9-9.2 mm and 1295-1400 rev/min for Fd_1, 6-10 mm and 720-1400 rev/min for Fd_2 and 9.8-10 mm and 1295-1400 rev/min for Fd_3, respectively. These results are fully consistent with those observed by Belaadi et al [28, 46] for epoxy/jute fabric biocomposites under identical cutting conditions. In the case where the drill diameter is kept constant, the *Fd* factor increases with increasing feed rate. On the other hand, by increasing the spindle speed, the delamination factor decreases. In general, Fd_1 ($\approx$ 1.12 to 1.89) produces lower *Fd* values than Fd_2 ($\approx$ 1.12 to 3.07) and Fd_3 ($\approx$ 1.01 to 2.02).

3.4 Prediction of the delamination factor by neural networks

The input layer integrates the data into the network model, and the output layer provides the response. For the prediction of the delamination factor, a multilayer perceptron consisting of an input layer, a hidden layer and an output layer was used. The ANN network was designed using the MATLAB Neural Network Toolbox. The use of neural network modeling offers a powerful solution capable of simulating the behavior of all nonlinear systems [67]. The ANN model training method in this investigation was based on the LM (Levenberg-Marquardt) algorithm, which associates both the principles of the quasi-Newton algorithm and steepest descent backpropagation, adapted to solve nonlinear least squares problems and curve adjustment. Of the total data, 80% and 75% of the datasets were chosen as training sets, and the remaining

datasets (20% and 25%) of the total data were used for testing and validation for Fd_1 and (Fd_2, Fd_3), respectively. For models Fd_1, Fd_2 and Fd_3, the input layer contains three neurons, the hidden layers contain ten, eleven and eleven neurons, and the output layer contains one neuron (**Figure 5**). The choice of the number of neurons in the hidden layers is based on the principle of reducing the error with an increasing number of hidden nodes [68]. **Table 7** shows the ANN architectures and the MSE and R-values for training, validation and testing of Fd_1, Fd_2 *and* Fd_3. In fact, these neurons are linked together by weights. **Figures 6 a-i** correspond to the predictions of *Fd* delamination through the neural network against the experimental test results for Fd_1, Fd_2 *and* Fd_3 for the training, test, and validation data sets. The ANN prediction is in perfect agreement with the experimental results. Thus, according to the results, the capability of the ANN models developed for Fd_1, Fd_2 *and* Fd_3 can satisfactorily interpret the data, and this approach is a good way to predict the delamination factor (**Table 8**). Furthermore, the results indicate that the model is an effective and applicable way to measure the delamination factor of composites made from jute/polyester fabric.

3.5 Comparison of the RSM and ANN models

Figure 7 and **Table 9** present a comparison of the results predicted by the ANN and RSM models with those obtained experimentally. Both models provide a satisfactory description of the experimentally obtained results. **Figures 8-10** show a comparison between the 3D surface plots of the delamination factor as a function of *f*, *N* and *d* of the composite obtained with the RSM and ANN models. Both models provide a satisfactory description of the experimentally obtained results. According to the results of **Figure 11**, the maximum absolute percentage of the error in the prediction by the ANN model of the delamination factors Fd_1, Fd_2 and Fd_3 is 6.99%, 8.71% and 4.89%, while by the RSM model, this percentage is 7.58%, 9.36% and 7.14%, respectively. Therefore, we can conclude that the ANN model provides a more accurate prediction than the RSM model. Since these error rates are low, we can say that the optimization process is appropriate and that the model predicts the responses with high accuracy.

3.6 Optimization of the responses

Figures 12 and **13** show the mapping and distribution of the desirability contour and ramp function for Fd_1, Fd_2 and Fd_3 and their combination in **Figure 13d**. Determining the cutting parameters and minimizing the delamination factors are the main objectives of the optimization. **Table 10** shows the cutting parameters used in the optimization process as well as the optimized values of the factors, and the responses obtained are shown in **Table 11**. The selection of the

10 trials was conducted because of the high desirability factor. These first 10 trials show that at a low feed rate, a small tool diameter and a high spindle speed, the reduction of the delamination factor is appropriate with desirability factors of 1.00, 0.98 and 1.00 for Fd_1, Fd_2 and Fd_3, respectively (**Figures 13a-c**). The optimal drilling conditions according to **Table 11** (f = 50 mm/min, N = 1085.89 rev/min and d = 5.00 mm) resulted in minimal delamination for Fd_1, Fd_2 and Fd_3 with the following values, i.e., 1.13, 1.23 and 1.02, respectively. To solve the optimization problem through the genetic algorithm (GA) and to find a minimum of the multivariable nonlinear constraint function (fmincon) using MATLAB software, the models generated with the ANN method were chosen. The results of this optimization of the input parameters and Fd_1, Fd_2 and Fd_3 are presented in **Table 12**. Indeed, these results show that the response parameters from the GA and fmincon produce almost similar values. Finally, a comparison of the response parameters Fd_1, Fd_2 and Fd_3 with those predicted by the GA and fmincon algorithms are 1.11, 1.15 and 1.01 for RSM, 1.04, 1.70 and 1.59 for the fmincon function and 1.10, 1.84 and 1.65 for the GA, respectively, thus validating the relevance of the models and the concordance of the results with those obtained by the GA and fmincon [28]**.**

4. Conclusion

The present study focuses on the optimization of the delamination factor during the orthogonal drilling of a material consisting of a bidirectional jute/polyester fabric matrix using the BSD tool. Models via artificial neural networks (ANNs) and the response surface methodology (RSM) were developed to predict the delamination factor determined by different methods. A three-level factorial design was applied to generate the input-output data used to develop the ANN and RSM models. The two models were compared in terms of the performance based on their predictive accuracy through the realization of the surface curves corresponding to the direct and interaction links of the parameters related to the drilling operations. The main conclusions drawn from the present study are as follows:

- From the effects of the interaction of the cutting parameters during the drilling process, it is apparent that the combination of a low feed rate and small tool diameter is necessary to reduce the delamination factor.
- The delamination factor is influenced by the diameter of the drill as well as the size of the feed rate, and the spindle speed has no influence on the delamination factor.
- The contributions of the different elements of the optimal drilling condition to Fd_1, Fd_2 and Fd_3 are the drill diameter (60.77%, 64.15% and 58.34%), feed rate (12.02%, 13.19% and 5.43%), and spindle speed (0.18%, 0.59% and 0.67%), respectively.

- This optimization is considered to be of good quality, as the overall desirability factor is 97%.
- The results of the predictive models and the experimental results are in perfect agreement.
- The percentage of the maximum absolute error for the ANN model prediction of the delamination factors Fd_1, Fd_2 and Fd_3 is 6.99%, 8.71%, and 4.89%, compared to 7.58%, 9.36%, and 7.14% for the RSM model, respectively.
- The agreement between the ANN and RSM models, used to predict cutting parameters in drilling processes, and the experimental data is very high. A comparison of the experimental results with those predicted by the RSM and ANN models reveals that the ANN models are more accurate and generate excellent results.

Acknowledgements : The authors gratefully acknowledge (la Direction Générale de la Recherche Scientifique et du Développement Technologique, Algérie) DGRSDT for their support in this work.

Author contribution

Bachir Adda : Conceptualization, Investigation, Methodology, Writing - review & editing.

Ahmed Belaadi: Conceptualization, Investigation, Methodology, Supervision, Writing - review & editing.

Messaouda Boumaaza: Conceptualization, Investigation, Writing - review & editing.

Mostefa Bourchak: Investigation, Writing - review & editing.

Funding information : The authors declare no funding information.

ORCID ID Ahmed Belaadi https://orcid.org/0000-0002-6059-3974

Data availability Not applicable.

COMPLIANCE WITH ETHICAL STANDARDS

Competing interests The authors declare no competing interests.

Ethics approval The work contains no libelous or unlawful statements, does not infringe on the rights of others, or contains material or instructions that might cause harm or injury.

Consent to participate The authors consent to participate.

Consent for publication The authors consent to publish.

References

1. Atagur M, Seki Y, Oncu O, et al (2020) Evaluating of reinforcing effect of Ceratonia Siliqua for polypropylene: Tensile, flexural and other properties. Polym Test 89:106607. https://doi.org/https://doi.org/10.1016/j.polymertesting.2020.106607
2. Sarasini F, Tirillò J, Lampani L, et al (2019) Static and dynamic characterization of agglomerated cork and related sandwich structures. Compos Struct 212:439–451. https://doi.org/10.1016/j.compstruct.2019.01.054
3. Belaadi A, Bourchak M, Aouici H (2016) Mechanical properties of vegetal yarn: Statistical approach. Compos Part B Eng 106:. https://doi.org/10.1016/j.compositesb.2016.09.033
4. Belaadi A, Amroune S, Bourchak M (2019) Effect of eco-friendly chemical sodium bicarbonate treatment on the mechanical properties of flax fibres: Weibull statistics. Int J Adv Manuf Technol. https://doi.org/10.1007/s00170-019-04628-8
5. Zhou Y, Fan M, Chen L (2016) Interface and bonding mechanisms of plant fibre composites: An overview. Elsevier Ltd
6. Rajmohan T, Vinayagamoorthy R, Mohan K (2019) Review on effect machining parameters on performance of natural fibre–reinforced composites (NFRCs). J Thermoplast Compos Mater 32:1282–1302. https://doi.org/10.1177/0892705718796541
7. Dutta S, Kim NK, Das R, Bhattacharyya D (2019) Effects of sample orientation on the fire reaction properties of natural fibre composites. Compos Part B Eng 157:195–206. https://doi.org/10.1016/j.compositesb.2018.08.118
8. Merli R, Preziosi M, Acampora A, et al (2020) Recycled fibers in reinforced concrete: A systematic literature review. J Clean Prod. https://doi.org/10.1016/j.jclepro.2019.119207
9. Cherief M, Belaadi A, Bouakba M, et al (2020) Behaviour of lignocellulosic fibre-reinforced cellular core under low-velocity impact loading: Taguchi method. Int J Adv Manuf Technol. https://doi.org/10.1007/s00170-020-05393-9
10. Boumaaza M, Belaadi A, Bourchak M (2020) The Effect of Alkaline Treatment on Mechanical Performance of Natural Fibers-reinforced Plaster: Optimization Using RSM. J Nat Fibers. https://doi.org/10.1080/15440478.2020.1724236
11. Jaouadi M, M'sahli S, Sakli F (2009) Optimization and Characterization of Pulp Extracted from the Agave Americana L. Fibers. Text Res J 79:110–120. https://doi.org/10.1177/0040517508090781
12. Bedjaoui A, Belaadi A, Amroune S, Madi B (2019) Impact of surface treatment of flax fibers on tensile mechanical properties accompanied by a statistical study. Int J Integr Eng 6:10–17
13. Lotfi A, Li H, Dao DV (2019) Effect of Drilling Parameters on Delamination and Hole Quality in Drilling Flax Fiber Reinforced Bio-Composites BT - Sustainable Design and Manufacturing 2018. In: Dao D, Howlett RJ, Setchi R, Vlacic L (eds). Springer International Publishing, Cham, pp 71–81

14. Lotfi A, Li H, Dao DV (2020) Analytical and experimental investigation of the parameters in drilling flax/poly(lactic acid) bio-composite laminates. Int J Adv Manuf Technol 109:503–521. https://doi.org/10.1007/s00170-020-05668-1
15. Benzannache N, Belaadi A, Boumaaza M, Bourchak M (2021) Improving the mechanical performance of biocomposite plaster/ Washingtonian filifira fibres using the RSM method. J Build Eng 33:. https://doi.org/10.1016/j.jobe.2020.101840
16. Benzidane R, Sereir Z, Bennegadi ML, et al (2018) Morphology, static and fatigue behavior of a natural UD composite: The date palm petiole 'wood.' Compos Struct 203:110–123. https://doi.org/10.1016/j.compstruct.2018.06.122
17. Djoudi T, Hecini M, Scida D, Djebloun Y (2019) Physico-Mechanical Characterization of Composite Materials Based on Date Palm Tree Fibers Physico-Mechanical Characterization of Composite Materials Based on Date Palm Tree Fibers. J Nat Fibers 0:1–14. https://doi.org/10.1080/15440478.2019.1658251
18. Mercy JL, Sivashankari P, Sangeetha M, et al (2020) Genetic Optimization of Machining Parameters Affecting Thrust Force during Drilling of Pineapple Fiber Composite Plates – an Experimental Approach. J Nat Fibers 1–12. https://doi.org/10.1080/15440478.2020.1788484
19. Zhang H, Zhu P, Liu Z, et al (2020) Research on prediction method of mechanical properties of open-hole laminated plain woven CFRP composites considering drilling-induced delamination damage. Mech Adv Mater Struct 0:1–16. https://doi.org/10.1080/15376494.2020.1745969
20. Feito N, Díaz-Álvarez J, López-Puente J, Miguelez MH (2018) Experimental and numerical analysis of step drill bit performance when drilling woven CFRPs. Compos Struct 184:1147–1155. https://doi.org/10.1016/j.compstruct.2017.10.061
21. Fernández-Pérez J, Cantero JL, Díaz-Álvarez J, Miguélez MH (2017) Influence of cutting parameters on tool wear and hole quality in composite aerospace components drilling. Compos Struct 178:157–161. https://doi.org/10.1016/j.compstruct.2017.06.043
22. Feito N, Diaz-Álvarez J, López-Puente J, Miguelez MH (2016) Numerical analysis of the influence of tool wear and special cutting geometry when drilling woven CFRPs. Compos Struct 138:285–294. https://doi.org/10.1016/j.compstruct.2015.11.065
23. Feito N, Diaz-Álvarez A, Cantero JL, et al (2016) Experimental analysis of special tool geometries when drilling woven and multidirectional CFRPs. J Reinf Plast Compos 35:33–55. https://doi.org/10.1177/0731684415612931
24. Díaz-Álvarez J, Olmedo A, Santiuste C, Miguélez MH (2014) Theoretical estimation of thermal effects in drilling of woven carbon fiber composite. Materials (Basel) 7:4442–4454. https://doi.org/10.3390/ma7064442
25. Díaz-Álvarez A, Rodríguez-Millán M, Díaz-Álvarez J, Miguélez MH (2018) Experimental analysis of drilling induced damage in aramid composites. Compos Struct 202:1136–1144. https://doi.org/10.1016/j.compstruct.2018.05.068

26. Bayraktar Ş, Turgut Y (2020) Determination of delamination in drilling of carbon fiber reinforced carbon matrix composites/Al 6013-T651 stacks. Measurement 154:107493. https://doi.org/https://doi.org/10.1016/j.measurement.2020.107493
27. Geng D, Liu Y, Shao Z, et al (2019) Delamination formation, evaluation and suppression during drilling of composite laminates: A review. Compos Struct 216:168–186. https://doi.org/https://doi.org/10.1016/j.compstruct.2019.02.099
28. Belaadi A, Laouici H, Bourchak M (2020) Mechanical and drilling performance of short jute fibre-reinforced polymer biocomposites: statistical approach. Int J Adv Manuf Technol 106:1989–2006. https://doi.org/10.1007/s00170-019-04761-4
29. Chaitanya S, Singh I (2018) Ecofriendly treatment of aloe vera fibers for PLA based green composites. Int J Precis Eng Manuf - Green Technol 5:143–150. https://doi.org/10.1007/s40684-018-0015-8
30. Bajpai PK, Singh I (2013) Drilling behavior of sisal fiber-reinforced polypropylene composite laminates. J Reinf Plast Compos 32:1569–1576. https://doi.org/10.1177/0731684413492866
31. Bajpai PK, Debnath K, Singh I (2015) Hole making in natural polylactic acid laminates : An experimental investigation. J Thermoplast Compos Mater 30:1–17. https://doi.org/10.1177/0892705715575094
32. Debnath K, Sisodia M, Kumar A, Singh I (2016) Damage-Free Hole Making in Fiber-Reinforced Composites: An Innovative Tool Design Approach. Mater Manuf Process 31:1400–1408. https://doi.org/10.1080/10426914.2016.1140191
33. Debnath K, Singh I, Dvivedi A (2014) Drilling Characteristics of Sisal Fiber-Reinforced Epoxy and Polypropylene Composites. Mater Manuf Process 29:1401–1409. https://doi.org/10.1080/10426914.2014.941870
34. Debnath K, Singh I, Dvivedi A (2017) On the analysis of force during secondary processing of natural fiber-reinforced composite laminates. Polym Compos 38:164–174. https://doi.org/10.1002/pc.23572
35. Chaudhary V, Gohil PP (2016) Investigations on Drilling of Bidirectional Cotton Polyester Composite. Mater Manuf Process 31:960–968. https://doi.org/10.1080/10426914.2015.1059444
36. Venkateshwaran N, ElayaPerumal A (2013) Hole quality evaluation of natural fiber composite using image analysis technique. J Reinf Plast Compos 32:1188–1197. https://doi.org/10.1177/0731684413486847
37. Athijayamani A, Thiruchitrambalam M, Natarajan U, Pazhanivel B (2010) Influence of alkali-treated fibers on the mechanical properties and machinability of roselle and sisal fiber hybrid polyester composite. Polym Compos 31:723–731. https://doi.org/10.1002/pc.20853
38. Ramesh M, Sri Ananda Atreya T, Aswin US, et al (2014) Processing and mechanical property evaluation of banana fiber reinforced polymer composites. Procedia Eng 97:563–572.

https://doi.org/10.1016/j.proeng.2014.12.284
39. Ismail SO, Dhakal HN, Dimla E, et al (2016) Effects of drilling parameters and aspect ratios on delamination and surface roughness of lignocellulosic HFRP composite laminates. J Appl Polym Sci 133:. https://doi.org/10.1002/app.42879
40. De Olveira LÁ, Santos JC Dos, Panzera TH, et al (2018) Investigations on short coir fibre-reinforced composites via full factorial design. Polym Polym Compos 26:391–399. https://doi.org/10.1177/0967391118806144
41. Abilash N, Sivapragash M (2016) Optimizing the delamination failure in bamboo fiber reinforced polyester composite. J King Saud Univ - Eng Sci 28:92–102. https://doi.org/https://doi.org/10.1016/j.jksues.2013.09.004
42. Díaz-Álvarez A, Díaz-Álvarez J, Santiuste C, Miguélez MH (2019) Experimental and numerical analysis of the influence of drill point angle when drilling biocomposites. Compos Struct 209:700–709. https://doi.org/10.1016/j.compstruct.2018.11.018
43. Babu GD, Babu KS, Gowd BUM (2012) Effects of drilling parameters on delamination of hemp fiber reinforced composites. Int J Mech Eng Res Dev 2:1–8
44. Azuan SAS (2013) Effects of Drilling Parameters on Delamination of Coconut Meat Husk Reinforced Polyester Composites. Adv Environ Biol 7:1097–1100. https://doi.org/10.1007/978-3-642-38345-8_6
45. Roy Choudhury M, Srinivas MS, Debnath K (2018) Experimental investigations on drilling of lignocellulosic fiber reinforced composite laminates. J Manuf Process 34:51–61. https://doi.org/https://doi.org/10.1016/j.jmapro.2018.05.032
46. Belaadi A, Boumaaza M, Amroune S, Bourchak M (2020) Mechanical characterization and optimization of delamination factor in drilling bidirectional jute fibre-reinforced polymer biocomposites. Int J Adv Manuf Technol. https://doi.org/10.1007/s00170-020-06217-6
47. Rao YS, Mohan NS, Shetty N, Shivamurthy B (2019) Drilling and structural property study of multi-layered fiber and fabric reinforced polymer composite - a review. Mater Manuf Process 34:1549–1579. https://doi.org/10.1080/10426914.2019.1686522
48. Azuan SAS, Juraidi JM, Muhamad WMW (2012) Evaluation of Delamination in Drilling Rice Husk Reinforced Polyester Composites. Appl Mech Mater 232:106–110. https://doi.org/10.4028/www.scientific.net/AMM.232.106
49. Aravindh S, Umanath K (2015) Delamination in drilling of natural Fibre Reinforced Polymer Composites produced by Compression moulding. Appl Mech Mater 767:796–800. https://doi.org/10.4028/www.scientific.net/AMM.766-767.796
50. Sridharan V, Muthukrishnan N (2013) Optimization of machinability of polyester/modified jute fabric composite using grey relational analysis (GRA). Procedia Eng 64:1003–1012. https://doi.org/10.1016/j.proeng.2013.09.177
51. Sridharan V, Raja T, Muthukrishnan N (2016) Study of the Effect of Matrix , Fibre Treatment

and Graphene on Delamination by Drilling Jute / Epoxy Nanohybrid Composite. Arab J Sci Eng 10–14. https://doi.org/10.1007/s13369-015-2005-2

52. Yallew TB, Kumar P, Singh I (2015) A study about hole making in woven jute fabric-reinforced polymer composites. Proc IMechE Part L J Mater Des Appl 0:1–11. https://doi.org/10.1177/1464420715587750
53. Monteiro SN, Terrones LAH, D'Almeida JRM (2008) Mechanical performance of coir fiber/polyester composites. Polym Test 27:591–595. https://doi.org/10.1016/j.polymertesting.2008.03.003
54. Jayabal S, Natarajan U (2011) Drilling analysis of coir – fibre-reinforced polyester composites. Bull Mater Sci 34:1563–1567. https://doi.org/doi.org/10.1007/s12034-011-0359-y
55. Durão LMP, Gonçalves DJS, Tavares JMRS, et al (2013) Drilling delamination outcomes on glass and sisal reinforced plastics. Mater Sci Forum 730–732:301–306. https://doi.org/10.4028/www.scientific.net/MSF.730-732.301
56. Çelik YH, Alp MS (2020) Determination of Milling Performance of Jute and Flax Fiber Reinforced Composites. J Nat Fibers 1–15. https://doi.org/10.1080/15440478.2020.1764435
57. Vinayagamoorthy R (2012) Analysis of cutting forces during milling of natural fibered composites using Fuzzy logic. Int J Compos Mater Manuf
58. Chegdani F, El M, Chebbi A (2021) Cutting behavior of flax fibers as reinforcement of biocomposite structures involving multiscale hygrometric shear. Compos Part B 211:108660. https://doi.org/10.1016/j.compositesb.2021.108660
59. Díaz-Álvarez A, Díaz-Álvarez J, Cantero JL, Santiuste C (2020) Analysis of orthogonal cutting of biocomposites. Compos Struct 234:111734. https://doi.org/https://doi.org/10.1016/j.compstruct.2019.111734
60. Chandramohan D, Rajesh S (2014) STUDY OF MACHINING PARAMETERS ON NATURAL FIBER PARTICLE REINFORCED POLYMER COMPOSITE MATERIAL. Acad J Manuf Eng 12:
61. Rezghi Maleki H, Hamedi M, Kubouchi M, Arao Y (2019) Experimental investigation on drilling of natural flax fiber-reinforced composites. Mater Manuf Process 34:283–292. https://doi.org/10.1080/10426914.2018.1532584
62. Nasir AAA, Azmi AI, Khalil ANM (2015) Parametric Study on the Residual Tensile Strength of Flax Natural Fibre Composites after Drilling Operation. Procedia Manuf 2:97–101. https://doi.org/https://doi.org/10.1016/j.promfg.2015.07.017
63. Davim JP, Reis P (2003) Drilling carbon fiber reinforced plastics manufactured by autoclave—experimental and statistical study. Mater Des 24:315–324. https://doi.org/https://doi.org/10.1016/S0261-3069(03)00062-1
64. Parthipan N, Ilangkumaran M, Maridurai T, Prasanna SC (2020) Effect of Silane Treated Silicon (IV) Oxide Nanoparticle Addition on Mechanical, Impact Damage and Drilling

Characteristics of Kenaf Fibre-Reinforced Epoxy Composite. Silicon 12:459–467. https://doi.org/10.1007/s12633-019-00138-0

65. Davim JP, Rubio JC, Abrao AM (2007) A novel approach based on digital image analysis to evaluate the delamination factor after drilling composite laminates. Compos Sci Technol 67:1939–1945. https://doi.org/https://doi.org/10.1016/j.compscitech.2006.10.009
66. Majumder A (2010) COMPARISON OF ANN WITH RSM IN PREDICTING SURFACE ROUGHNESS WITH RESPECT TO PROCESS PARAMETERS IN Nd: YAG LASER DRILLING. Int J Eng Sci Technol 2:5175–5186
67. Karnik SR, Gaitonde VN, Davim JP (2008) A comparative study of the ANN and RSM modeling approaches for predicting burr size in drilling. Int J Adv Manuf Technol 38:868–883
68. Benardos PG, Vosniakos G-C (2003) Predicting surface roughness in machining: a review. Int J Mach Tools Manuf 43:833–844. https://doi.org/https://doi.org/10.1016/S0890-6955(03)00059-2
69. Rezghi Maleki H, Hamedi M, Kubouchi M, Arao Y (2019) Experimental study on drilling of jute fiber reinforced polymer composites. J Compos Mater 53:283–295
70. Ramesh M, Palanikumar K, Reddy KH (2014) Experimental investigation and analysis of machining characteristics in drilling hybrid glass-sisal-jute fiber reinforced polymer composites. In: 5th international & 26th all india manufacturing technology, design and research conference AIMTDR
71. Vinayagamoorthy R, Rajeswari N, Karthikeyan S (2015) Investigations of damages during drilling of natural sandwich composites. In: Applied Mechanics and Materials. Trans Tech Publ, pp 812–817
72. Vinayagamoorthy R, Rajeswari N, Sivanarasimha S, Balasubramanian K (2015) Fuzzy based optimization of thrust force and torque during drilling of natural hybrid composites. In: Applied Mechanics and Materials. Trans Tech Publ, pp 265–269
73. Ramnath BV, Sharavanan S, Jeykrishnan J (2017) Optimization of process parameters in drilling of fibre hybrid composite using Taguchi and grey relational analysis. In: IOP Conference Series: Materials Science and Engineering. IOP Publishing, p 12003
74. Vinayagamoorthy R (2017) Parametric optimization studies on drilling of sandwich composites using the Box–Behnken design. Mater Manuf Process 32:645–653. https://doi.org/10.1080/10426914.2016.1232811
75. Pailoor S, Murthy HNN, Sreenivasa TN (2021) Drilling of In-Line Compression Molded Jute / Polypropylene Composites. J Nat Fibers 18:91–104. https://doi.org/10.1080/15440478.2019.1612309
76. Babu J, Sunny T, Paul NA, et al (2016) Assessment of delamination in composite materials: A review. Proc Inst Mech Eng Part B J Eng Manuf 230:1990–2003. https://doi.org/10.1177/0954405415619343

77. Vigneshwaran S, John KM, Deepak Joel Johnson R, et al (2020) Conventional and unconventional machining performance of natural fibre-reinforced polymer composites: A review. J Reinf Plast Compos. https://doi.org/10.1177/0731684420958103
78. Mohan NS, Kulkarni SM, Ramachandra A (2007) Delamination analysis in drilling process of glass fiber reinforced plastic (GFRP) composite materials. J Mater Process Technol 186:265–271. https://doi.org/10.1016/j.jmatprotec.2006.12.043
79. Mudhukrishnan M, Hariharan P, Palanikumar K (2020) Measurement and analysis of thrust force and delamination in drilling glass fiber reinforced polypropylene composites using different drills. Meas J Int Meas Confed 149:106973. https://doi.org/10.1016/j.measurement.2019.106973
80. Chen W-C (1997) Some experimental investigations in the drilling of carbon fiber-reinforced plastic (CFRP) composite laminates. Int J Mach Tools Manuf 37:1097–1108. https://doi.org/https://doi.org/10.1016/S0890-6955(96)00095-8

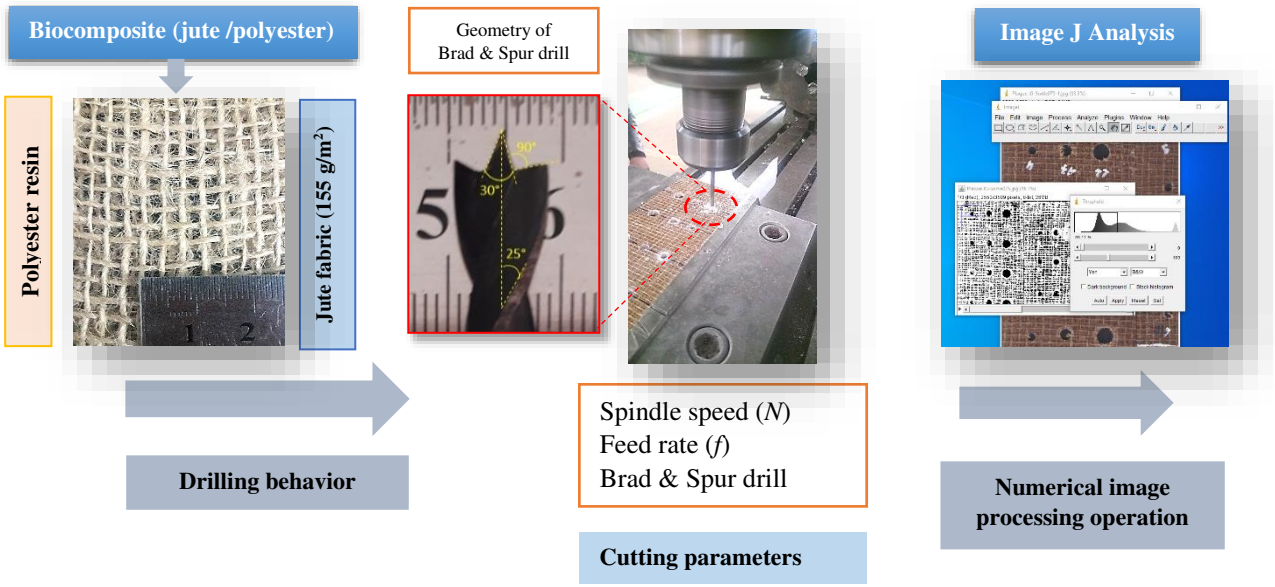

Figure 1: Schematic arrangement of experimental setup.

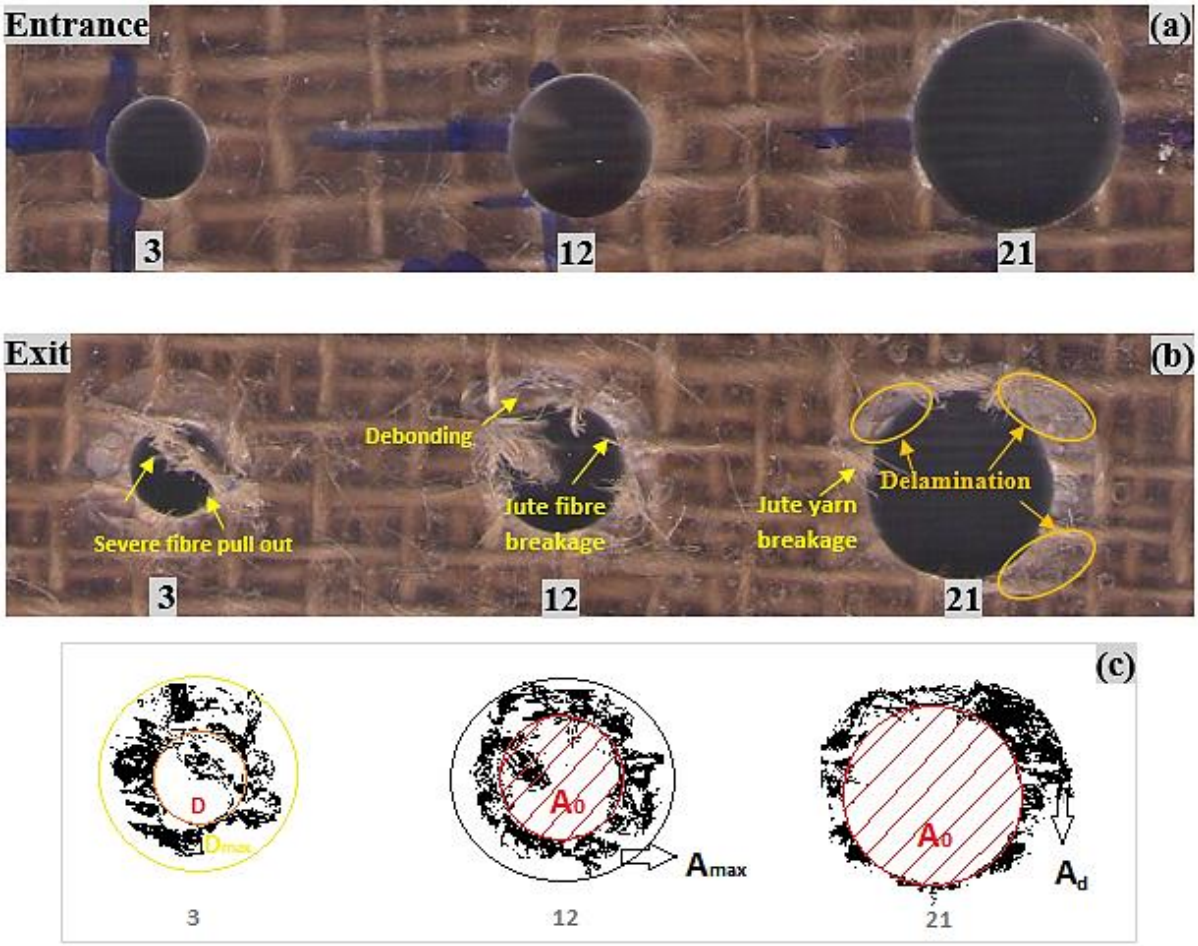

Figure 2. Typical holes drilled on jute fabric/polyester biocomposites for three test (#3, #12 and #21): (a) entrance, (b) exit and typical damage in drilling and (c) determination of different parameters for calculation the delamination factors at the drill and resulting image obtained with ImageJ software.

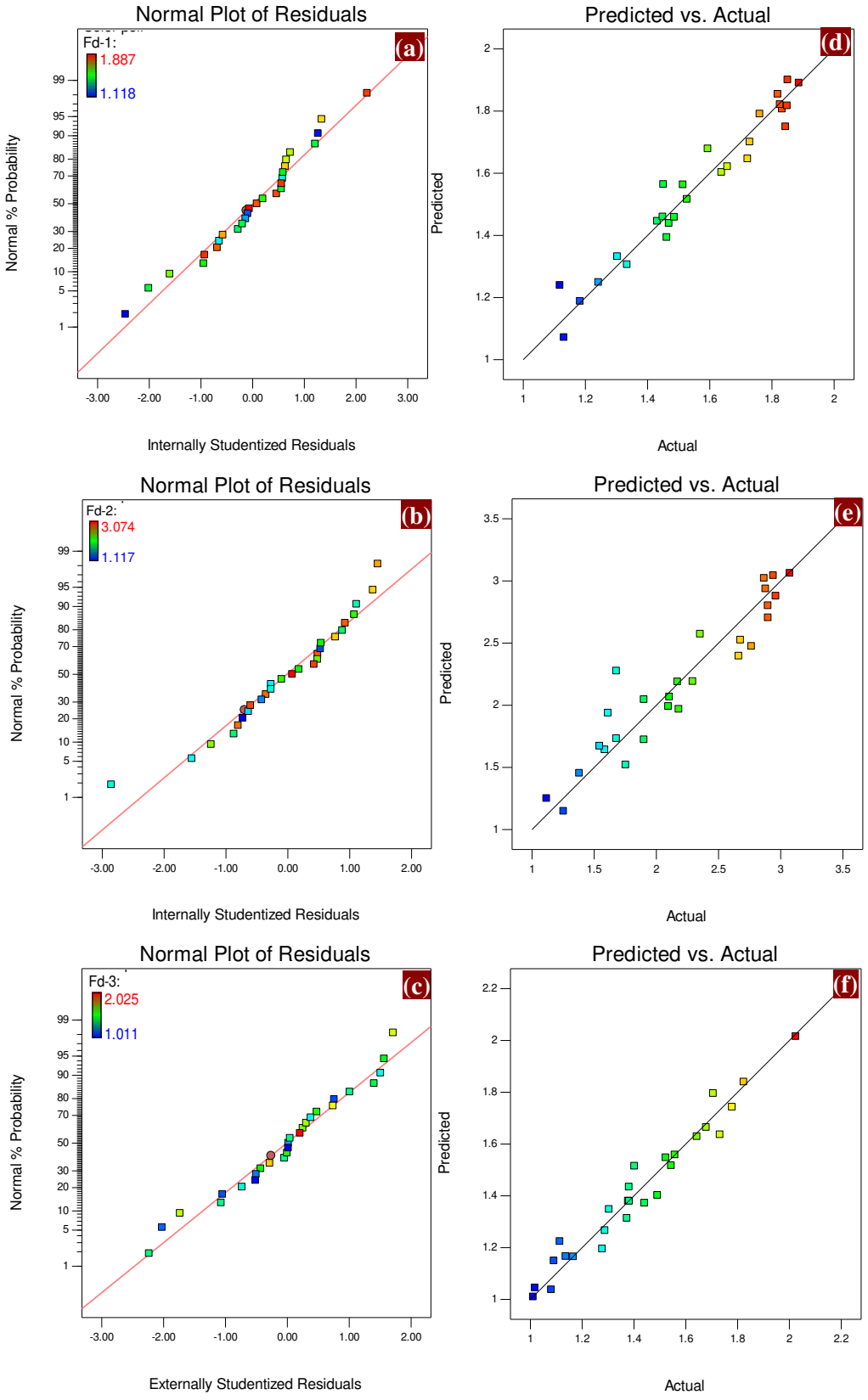

Figure. 3 (a–c) Normal probability distribution and (d–f) predicted vs. actual values for different F_d method evaluated.

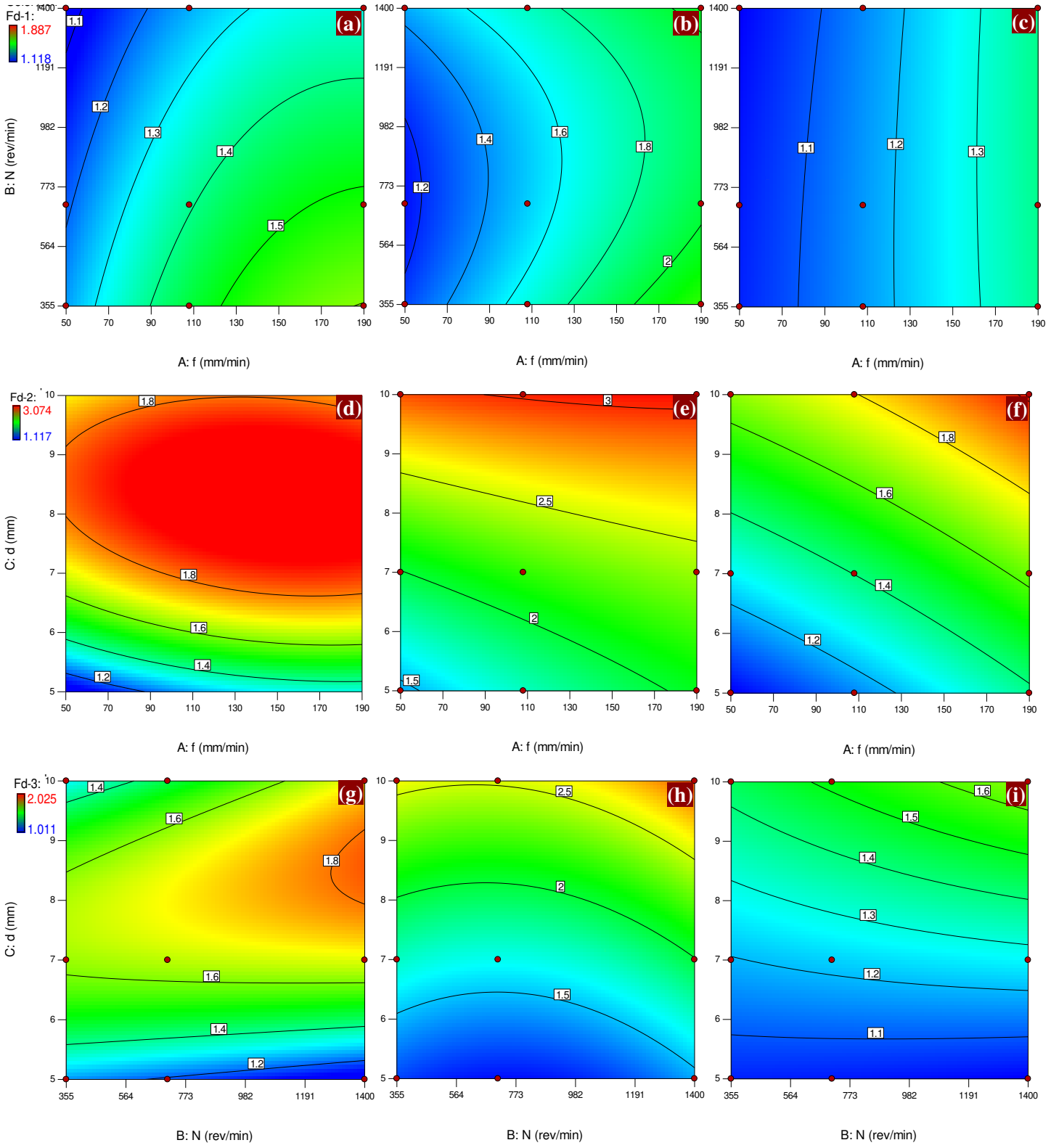

Figure 4 : Contour plots for predicted data of the different Fd evaluated as a function of the cutting parameters of the biocomposites produced: (a-c) *Fd1* data, (d-f) *Fd2* data et (g-i) *Fd3* data.

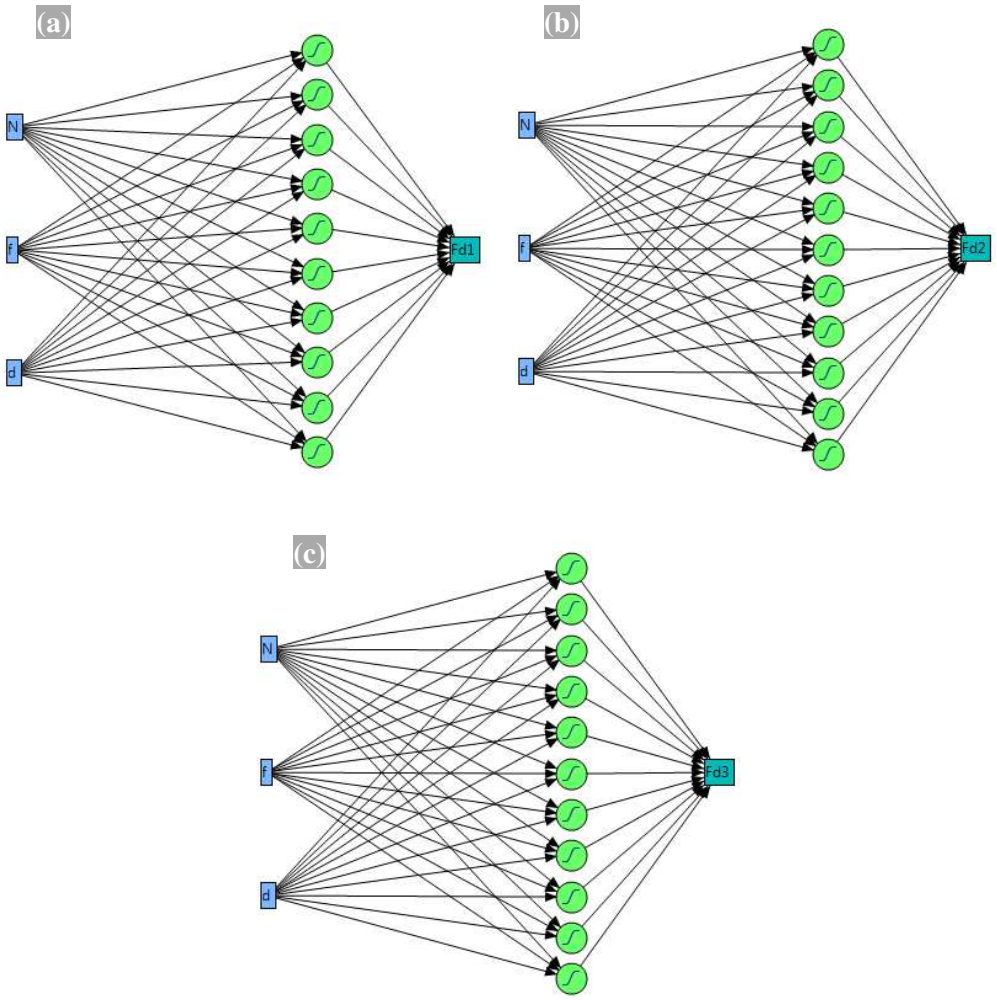

Fig. 5 ANN architecture used for (a) Fd_1, (b) Fd_2 and (b) Fd_3.

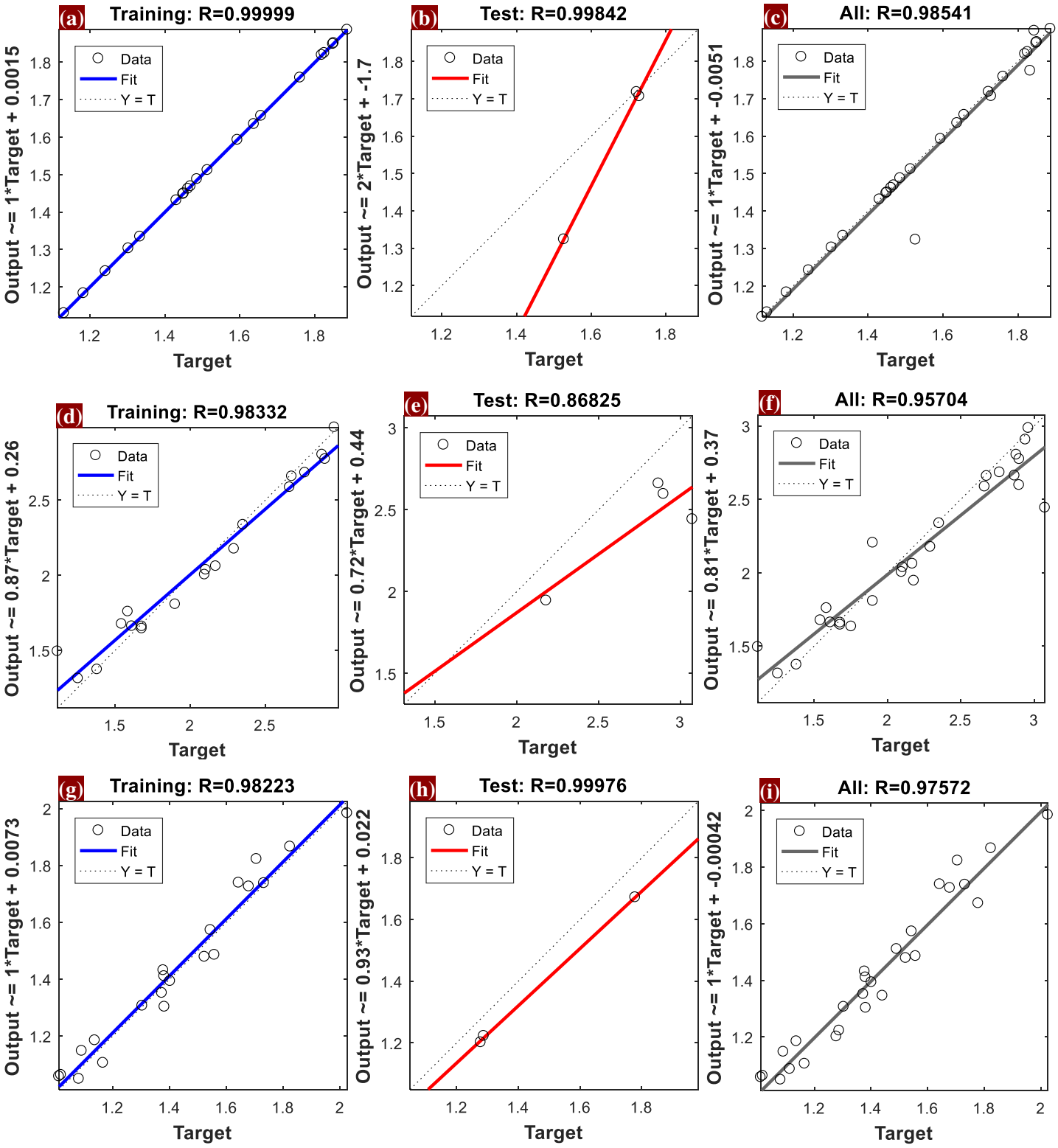

Fig. 6: Regression validation scheme of (a-c) Fd_1 data, (d-f) Fd_2 data et (g-i) Fd_3 data.

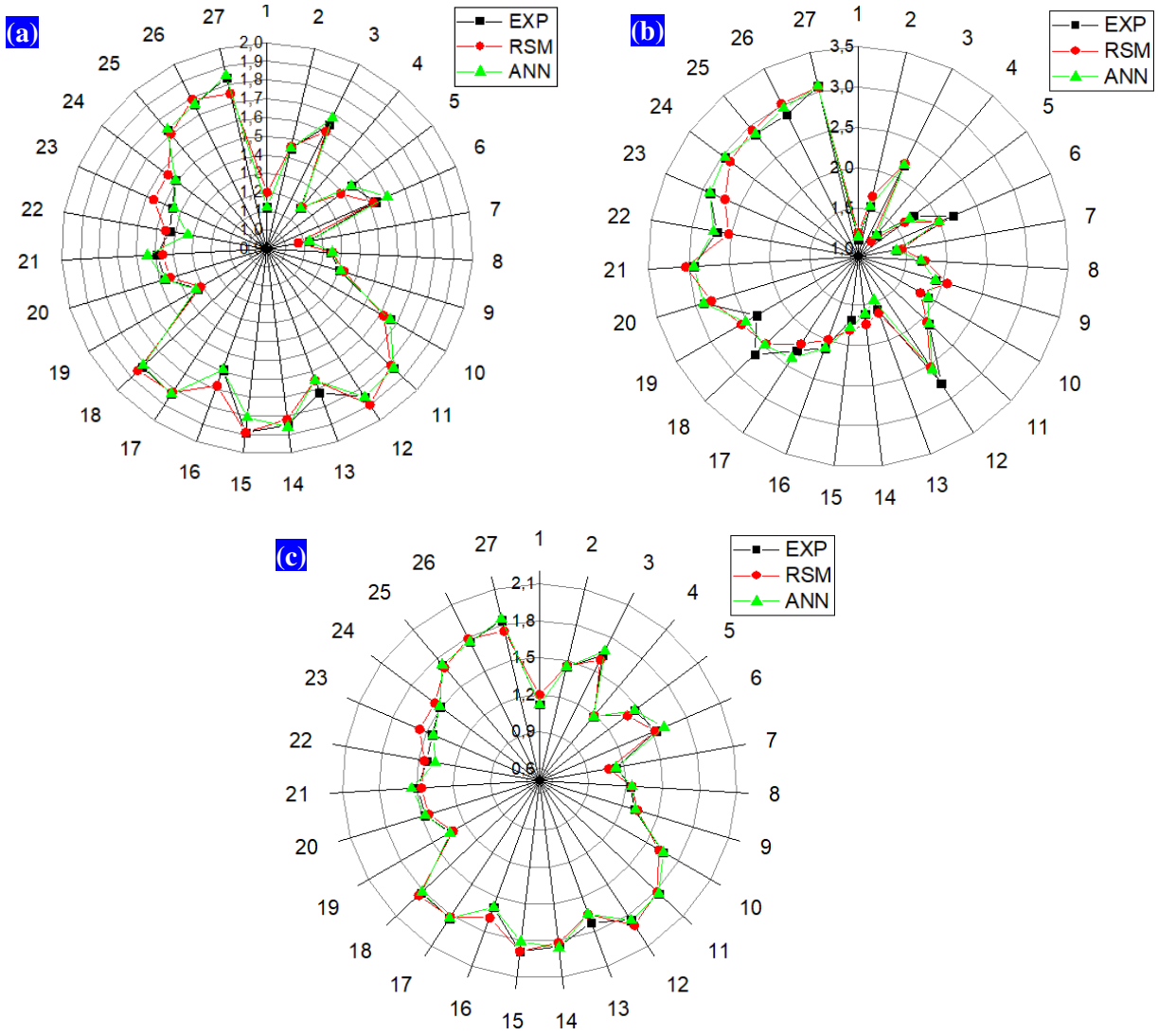

Figure 7 : Comparison between experimental and predicted Fd with RSM and ANN models (a) Fd_1 data, (b) Fd_2 data and (b) Fd_3 data.

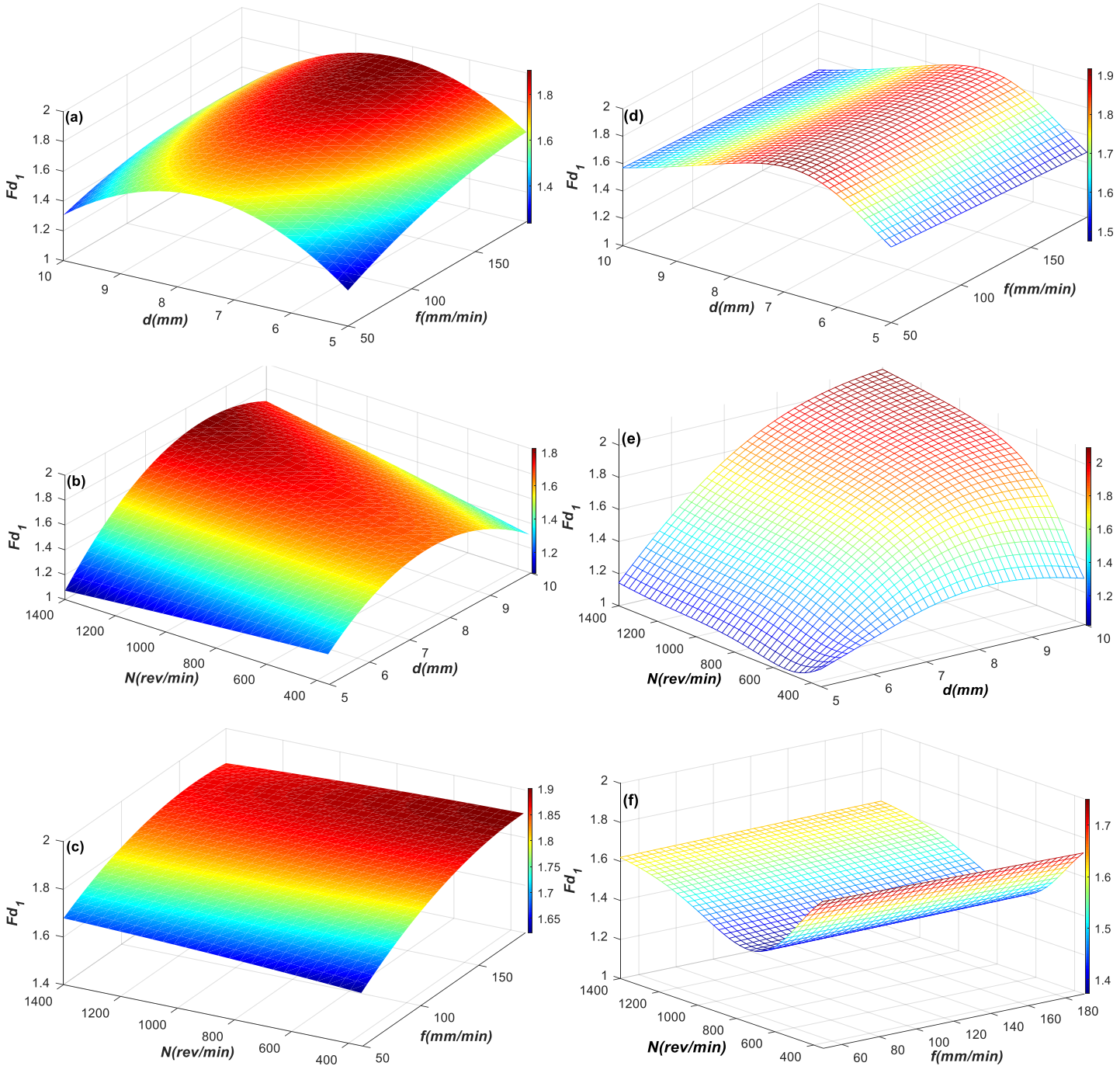

Figure 8 : Comparison between 3D surface plots of delamination factor for Fd_1 versus f, N and d of biocomposites elaborated (a-c) RSM and (d-f) ANN models.

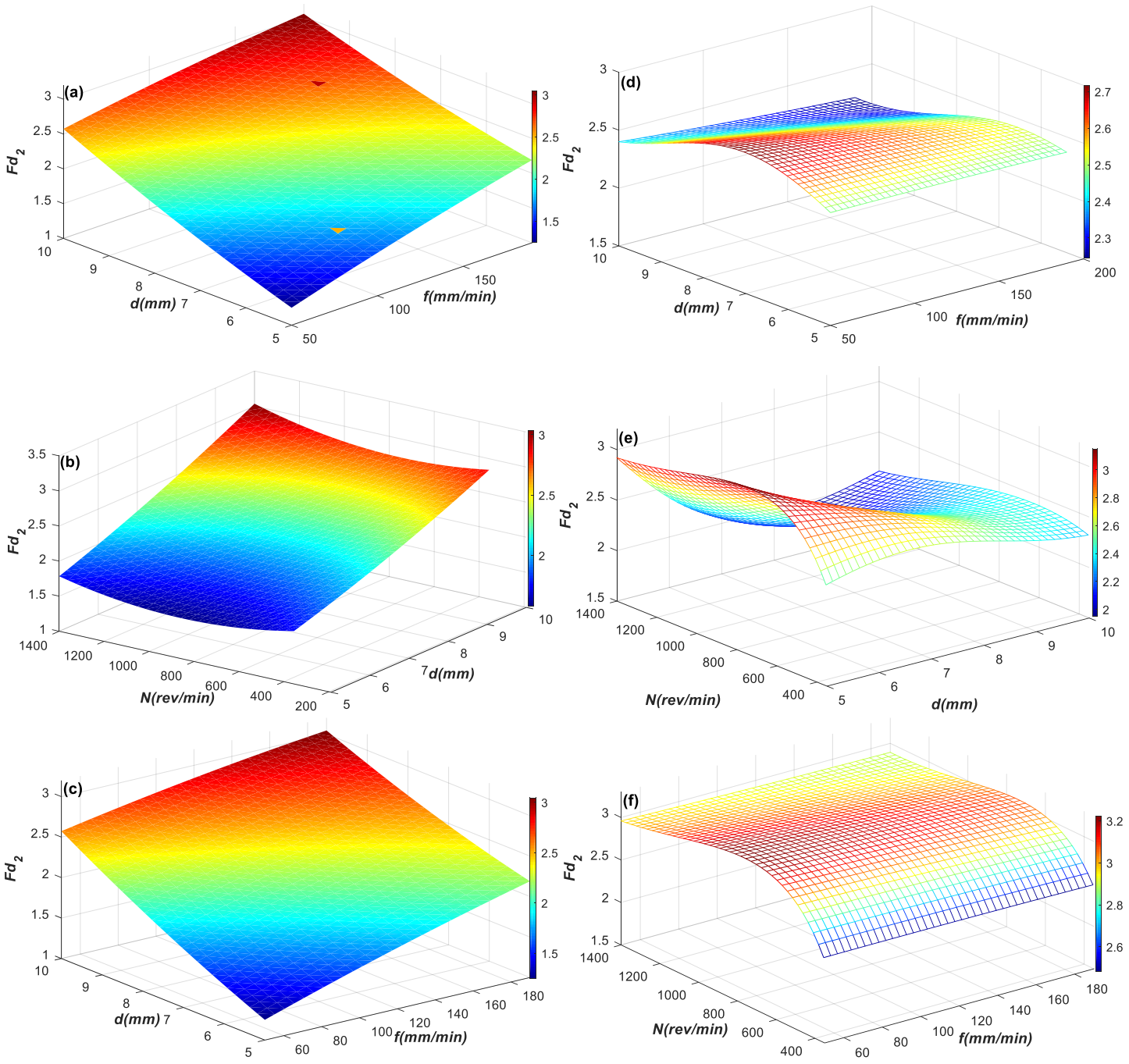

Figure 9 : Comparison between 3D surface plots of delamination factor for Fd_2 versus f, N and d of biocomposites elaborated (a-c) RSM and (d-f) ANN models.

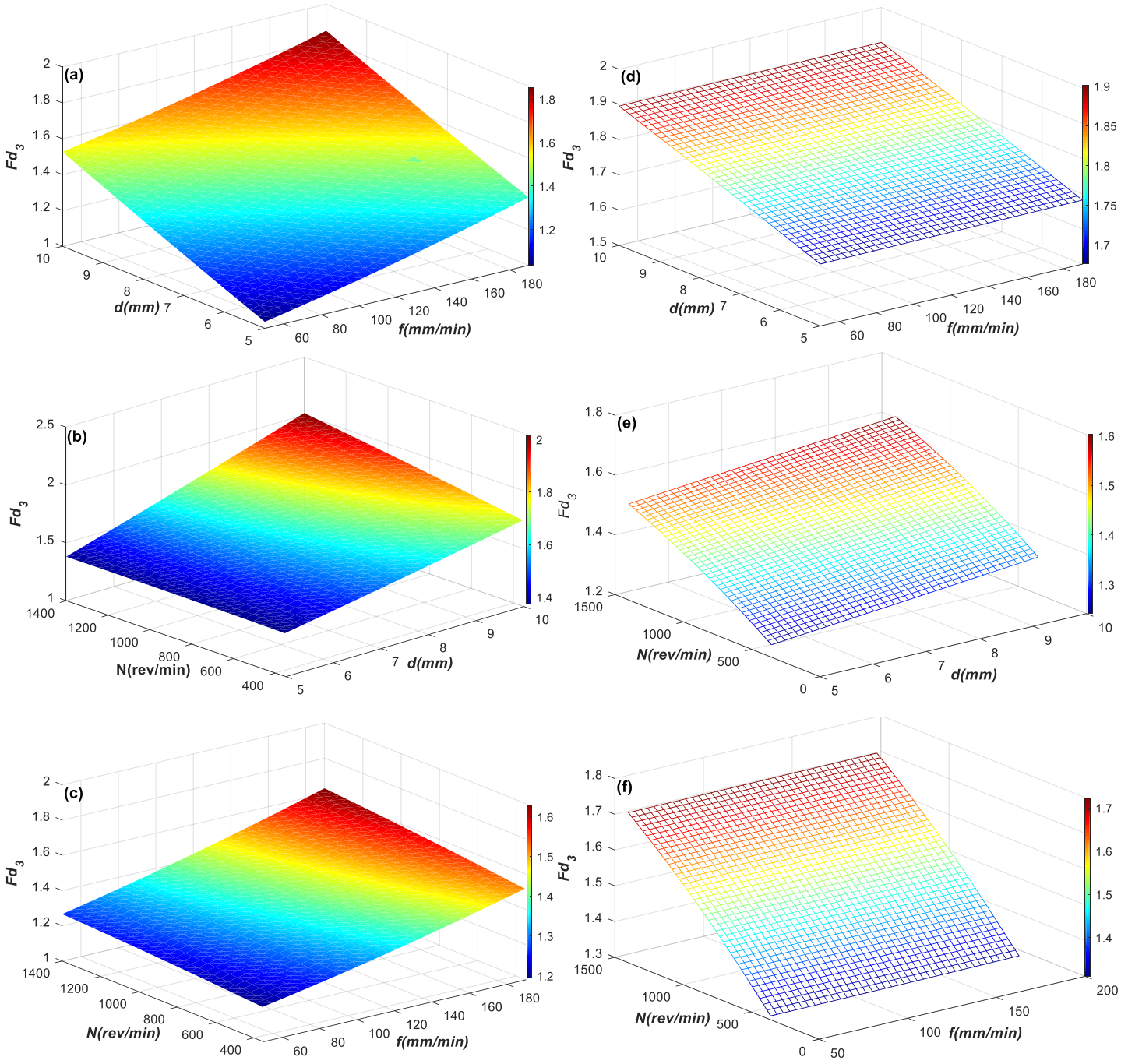

Figure 10 : Comparison between 3D surface plots of delamination factor for *Fd3* versus f, N and d of biocomposites elaborated (a-c) RSM and (d-f) ANN models.

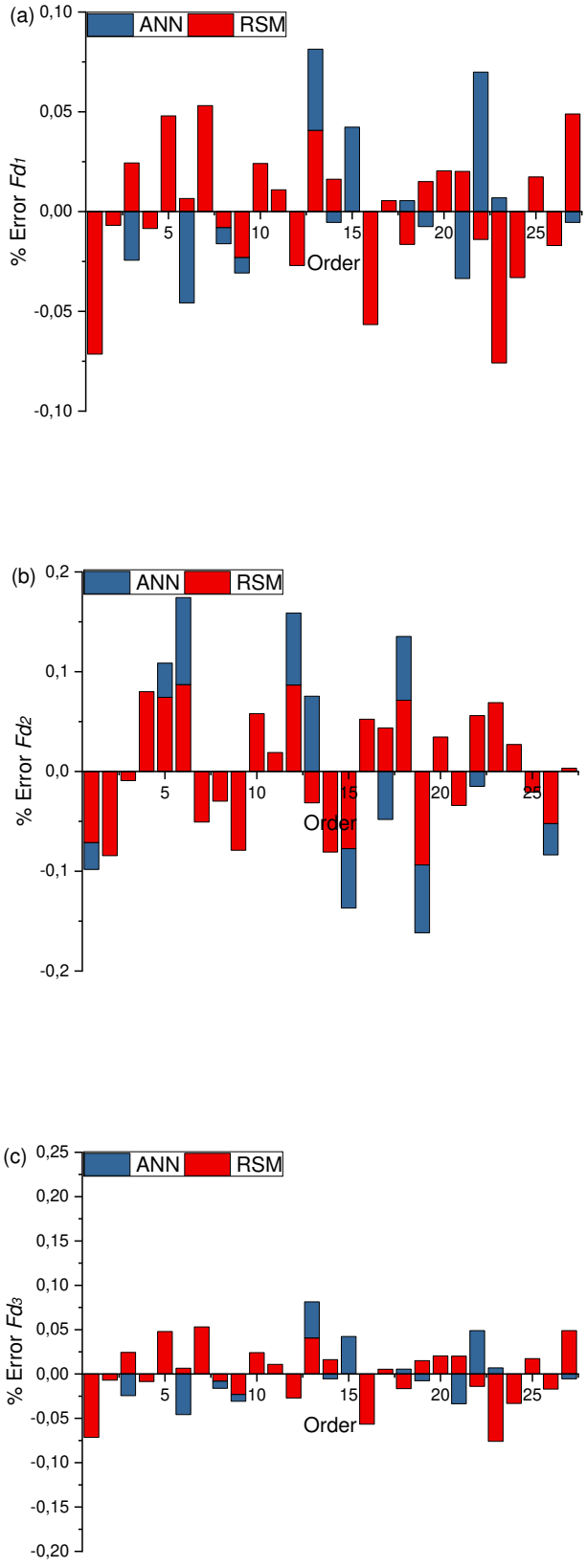

Figure 11. *Fd* residuals for RSM and ANN (a) *Fd1* data, (b) *Fd2* data and (b) *Fd3* data.

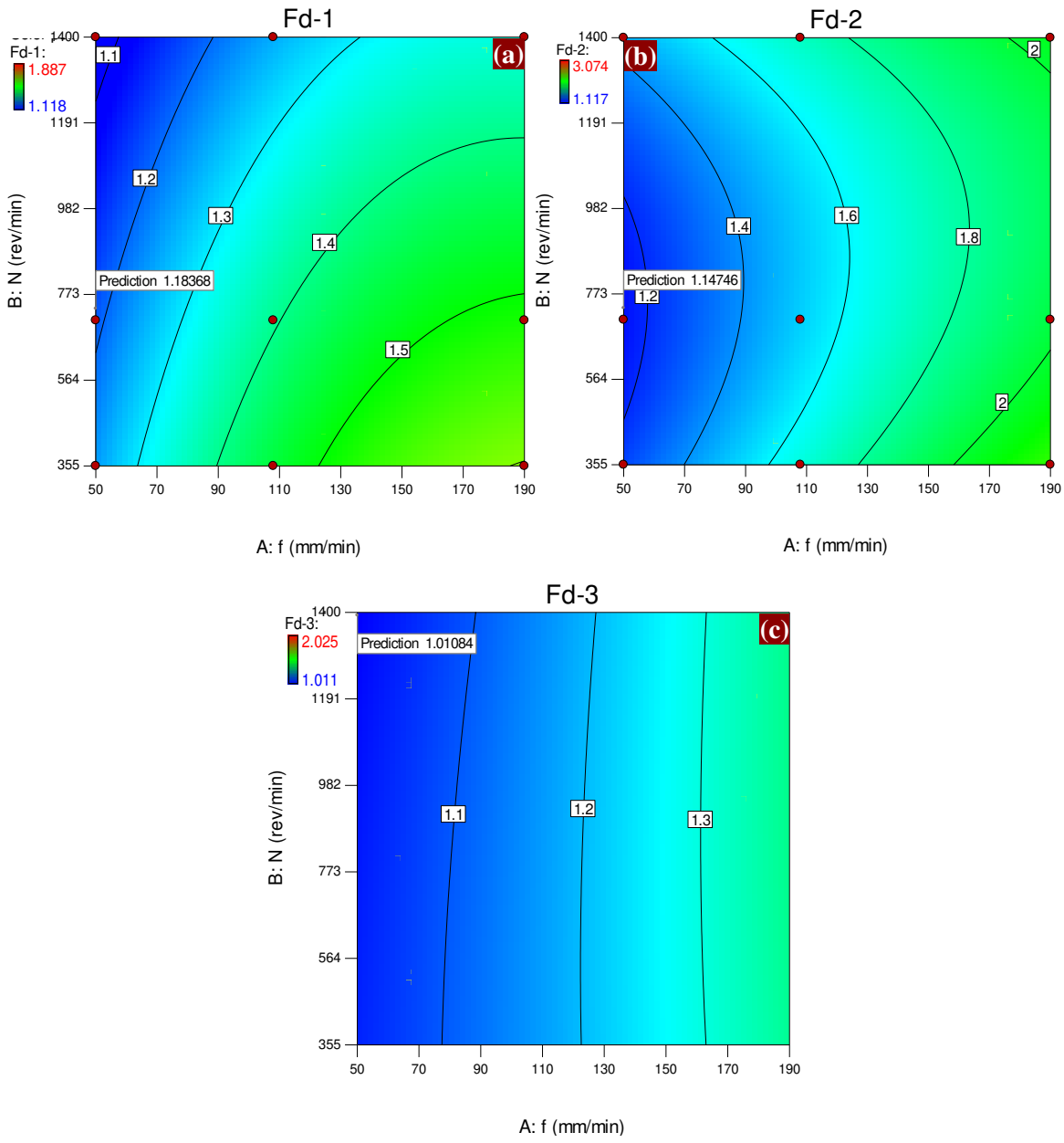

Figure 12: Contour plot of desirability for different *Fd* method evaluated.

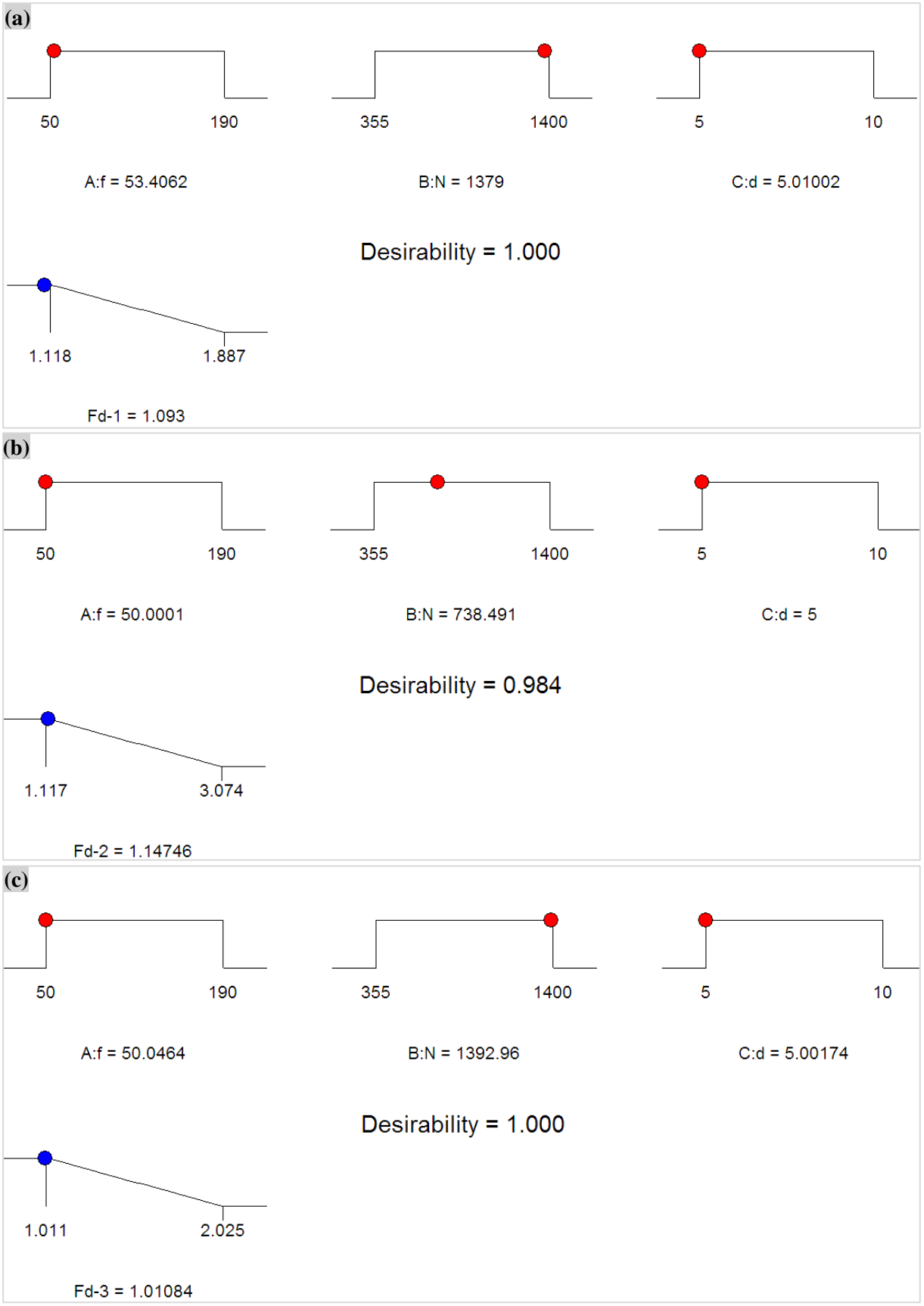
(a)
50
190
355
1400
5
10
A:f = 53.4062
B:N = 1379
C:d = 5.01002
Desirability = 1.000
1.118
1.887
Fd-1 = 1.093
(b)
50
190
355
1400
5
10
A:f = 50.0001
B:N = 738.491
C:d = 5
Desirability = 0.984
1.117
3.074
Fd-2 = 1.14746
(c)
50
190
355
1400
5
10
A:f = 50.0464
B:N = 1392.96
C:d = 5.00174
Desirability = 1.000
1.011
2.025
Fd-3 = 1.01084

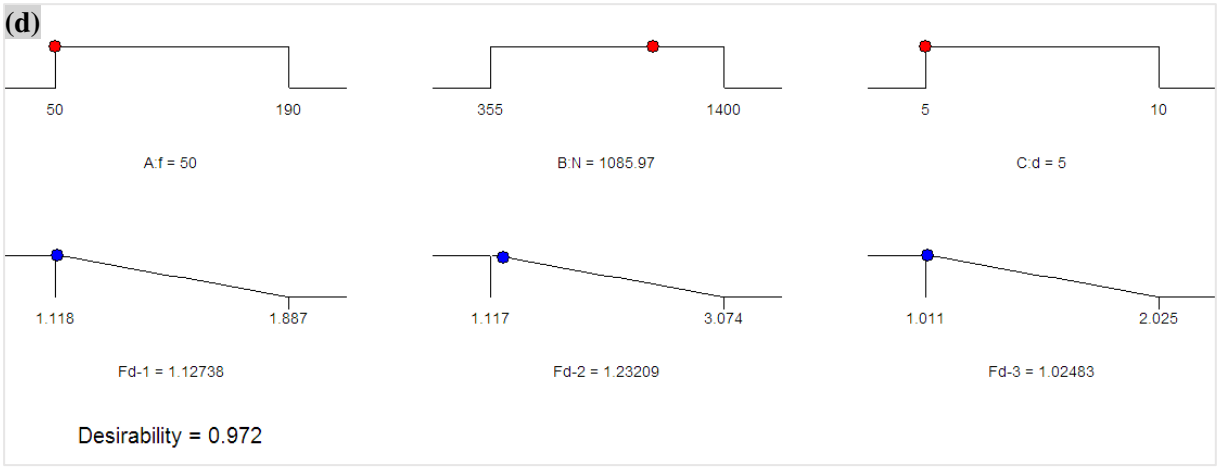

Figure 13. Ramp function graph of multi-objective optimization for different Fd method evaluated (a) Fd_1 data, (b) Fd_2 data, (c) Fd_3 data and (d) Combination data

Table 1 Process parameters available in open literature for drilling of jute fibre-reinforced polymer composites

Matrix	Fibre	**Fibre content (% w/w)**	Cutting parameters				References
			Tool material	**Drill diameter d (mm)**	**Feed rate f (mm/rev)**	**Spindle Speed N (rpm)**	
Epoxy	Unidirectional Jute	-	HSS twist drills	6, 8, 10	50, 150, 250 (mm/min)	1000, 2000, 3000	[49]
Polyester	Treated and untreated Jute fabric	30	HSS twist drill	6	0,03, 0,06, 0,09, 0,12	9,42, 15,07, 20,72, 26,36 (m/min)	[50]
Epoxy and Polyester	Treated and untreated Jute fabric	30	HSS twist drill	6	0,03, 0,06, 0,09, 0,12	500, 800, 1100, 1400	[51]
Polypropylene	Jute fabric	30, 40, 50	Twist drills Jo drills, parabolic drills	8	0,05, 0,12, 0,19	900, 1800 2800	[52]
Epoxy	Jute fabric	43	HSS twist drill CoroDrill 854, N_2OC CoroDrill 856, N_2OC	8	0,05, 0,10, 0,15	750, 1250, 1750	[69]
Polyester	Glass-sisal-jute	-	Brad & Spur, coated carbide	6, 9, 12	0,04, 0,06, 0,08	1000, 2000, 3000	[70]
Vinyl-ester	Untreated Vetiver- jute-glass	-	Twist drills, 60°, 90°,120°, 150°	10	0,1, 0,2, 0,3, 0,4	500, 1000, 1500, 2000	[71]
Vinyl-ester	Treated (NaOH) Vetiver- jute-glass	-	Twist drills, 60°, 90°,120°, 150°	10	0,1, 0,2, 0,3, 0,4	500, 1000, 1500, 2000	[72]
Epoxy	Glass-flax-jute		Drill bit carbide	6, 8, 10	0,1, 0,2, 0,3	600, 1200 1800	[73]
Polyester	Short jute fibre 5, 10 and 15 mm	40	Brad & Spur drills Twist drills	5, 7, 10	50, 108, 190 (mm/min)	355, 710, 1400	[28]
Epoxy	Jute fabric (210 g/m^2)	40	Brad & Spur drills Twist drills (HSS) Twist drills (HSS-TiN)	5, 7, 10	50, 108, 190 (mm/min)	355, 710, 1400	[46]
Polyester	Jute fabric and steel fibres		HSS, 90°,120°,150°	8,10,12	0,1, 0,2, 0,3	500, 1250, 2000	[74]
Polypropylene	Unidirectional Jute	30	HSS, Co-HSS	2, 3, 4	0,1, 0,2, 0,3	600, 1260 2700	[75]
Epoxy	Jute and flax fabric	-	HSS, HSS-TiN, WC	4	0,01, 0,015, 0,020	2500, 5000, 7500	[56]
Polyester	**Jute fabric (155 g/m^2)**	**30**	**Brad & Spur drills**	**5, 7, 10**	**50, 108, 190 (mm/min)**	**355, 710, 1400**	**This work**

CS: solid carbide; CSC: TiN coated solid carbide; HSS: High-speed steel; Brad & Spur drill: BSD

Table 2. Different delamination measuring equations [76–80].

Method estimation	Assessment parameter	Formula
Fd_1	Delamination factor (diameter)	$F_d = \frac{D_{max}}{D}$
Fd_2	Delamination factor (area)	$F_d = \frac{A_{max}}{A_0}$
Fd_3	Delamination factor (area)	$F_d = \frac{A_d}{A_0}$

A_0: drilled area (hole area)	D: nominal diameter of drilled hole
A_d: delamination area in the vicinity of the drilled hole	D_{max}: maximum diameter of delamination
A_{max} : delamination area related to D_{max}	F_d : conventional delamination factor

Table 3. Experimental results for delamination factor of the drilled holes at the exit.

Experiment number	Input variables			Output variables		
	f (mm/min)	N (rev/min)	d (mm)	Fd_1	Fd_2	Fd_3
1	50	355	5	1.12	1.12	1.02
2	108	355	5	1.45	1.54	1.14
3	190	355	5	1.64	2.17	1.44
4	50	710	5	1.18	1.25	1.08
5	108	710	5	1.46	1.75	1.17
6	190	710	5	1.53	2.18	1.38
7	50	1400	5	1.13	1.38	1.01
8	108	1400	5	1.24	1.68	1.09
9	190	1400	5	1.30	1.90	1.38
10	50	355	7	1.66	1.90	1.28
11	108	355	7	1.83	2.11	1.37
12	190	355	7	1.85	2.77	1.40
13	50	710	7	1.72	1.59	1.11
14	108	710	7	1.85	1.61	1.30
15	190	710	7	1.89	1.68	1.56
16	50	1400	7	1.59	2.10	1.29
17	108	1400	7	1.83	2.29	1.49
18	190	1400	7	1.82	2.66	1.64
19	50	355	10	1.33	2.35	1.38
20	108	355	10	1.47	2.90	1.52
21	190	355	10	1.49	2.94	1.78
22	50	710	10	1.43	2.68	1.54
23	108	710	10	1.45	2.90	1.73
24	190	710	10	1.51	2.96	1.82
25	50	1400	10	1.73	2.88	1.68
26	108	1400	10	1.76	2.87	1.71
27	190	1400	10	1.84	3.07	2.02

Table 4. Design of experiments.

n°	Factors	Notation	Units	Levels		
				L_1	L_2	L_3
1	Spindle speed	N	rev/min	355	710	1400
2	Feed rate	f	mm/min	50	108	190
3	Drill diameter	d	mm	5	7	10

Table 5. Mathematical models for different delamination factors for drilling of jute fabric /polyester biocomposite.

RSM response	
Fd_1	$-1.90932 + 7.86866 \times 10^{-3} \times f - 6.23020 \times 10^{-4} \times N + 0.87873 \times d - 7.06429 \times 10^{-7} \times f \times N - 3.01359 \times 10^{-4} \times f \times d + 1.07601 \times 10^{-4} \times N \times d - 1.46448 \times 10^{-5} \times f^2 - 2.28431 \times 10^{-8} \times N^2 - 0.059233 \times d^2$
Fd_2	$0.12200 + 0.012543 \times f - 1.07049 \times 10^{-3} \times N + 0.14591 \times d - 2.36589 \times 10^{-6} \times f \times N - 6.67351 \times 10^{-4} \times f \times d + 3.07495 \times 10^{-5} \times N \times d - 6.93560 \times 10^{-6} \times f^2 + 7.00806 \times 10^{-7} \times N^2 + 9.40370 \times 10^{-3} \times d^2$
Fd_3	$0.70471 + 1.64052 \times 10^{-3} \times f - 2.69733 \times 10^{-4} \times N + 0.047514 \times d + 2.92946 \times 10^{-7} \times f \times N - 2.6833 \times 10^{-5} \times f \times d + 5.07080 \times 10^{-5} \times N \times d - 3.02775 \times 10^{-6} \times f^2 - 1.81812 \times 10^{-8} \times N^2 + 9.11111 \times d^2$

Table 6. ANOVA for the response surface quadratic model for different delamination factors.

Source	DF	SS	MS	F-value	P-value	Cont. %	Remarks
a) ANOVA for delamination factor Fd_1							
Model	9	1.41	0.16	36.46	< 0.0001		Significant
f	1	*0.19*	*0.19*	*43.47*	*< 0.0001*	12.02	Significant
N	1	*0.017*	*0.017*	*3.94*	*0.0634*	0.18	
d	1	*0.26*	*0.26*	*60.12*	*< 0.0001*	60.77	Significant
f × *N*	1	*8.367E-003*	*8.367E-003*	*1.94*	*0.1814*	0.09	
f×*d*	1	*0.034*	*0.034*	*7.93*	*0.0119*	0.36	Significant
N×*d*	1	*0.25*	*0.25*	*57.66*	*< 0.0001*	2.66	Significant
f×*f*	1	*0.029*	*0.029*	*6.69*	*0.0192*	0.31	Significant
N×*N*	1	*1.816E-004*	*1.816E-004*	*0.042*	*0.8398*	0.00	
d×*d*	1	*0.75*	*0.75*	*173.57*	*< 0.0001*	7.98	Significant
Error	17	0.073	4.309E-003				
Total	26	1.49					
SD= 0.066 Mean = 1.56 Coefficient of variation = 4.21% Predicted residual error of sum of squares (PRESS) = 0.21						R^2= 95.07% R^2 adjusted = 92.47% R^2 predicted = 85.60% Adequate precision = 20.749	
c) ANOVA for delamination factor Fd_2							
Model	9	8.38	0.93	15.61	< 0.0001		Significant
f	1	*1.24*	*1.24*	*20.83*	*0.0003*	13.19	Significant
N	1	*0.055*	*0.055*	*0.92*	*0.3515*	0.59	
d	1	*6.03*	*6.03*	*100.99*	*< 0.0001*	64.15	Significant
f× *N*	1	*0.094*	*0.094*	*1.57*	*0.2268*	1.00	
f×*d*	1	*0.17*	*0.17*	*2.81*	*0.1122*	1.81	
N×*d*	1	*0.020*	*0.020*	*0.34*	*0.5675*	0.21	
f×*f*	1	*6.465E-003*	*6.465E-003*	*0.11*	*0.7461*	0.07	
N× *N*	1	*0.17*	*0.17*	*2.86*	*0.1088*	1.81	
d×*d*	1	*0.019*	*0.019*	*0.32*	*0.5814*	0.20	
Error	17	1.01	0.060				
Total	26	9.40					
SD= 0.24 Mean 2.19 Coefficient of variation = 11.13% Predicted residual error of sum of squares (PRESS) = 2.25						R^2= 89.21% R^2 adjusted = 83.49% R^2 predicted = 76.07% Adequate precision = 12.8777	
c) ANOVA for delamination factor Fd_3							
Model	9	1.77	0.20	41.58	< 0.0001		Significant
f	1	*0.51*	*0.51*	*106.87*	*< 0.0001*	5.43	Significant
N	1	*0.063*	*0.063*	*13.29*	*0.0020*	0.67	Significant
d	1	*1.16*	*1.16*	*244.16*	*< 0.0001*	58.34	Significant
f× *N*	1	*1.439E-003*	*1.439E-003*	*0.30*	*0.5887*	0.02	
f×*d*	1	*2.708E-004*	*2.708E-004*	*0.057*	*0.8139*	0.00	
N×*d*	1	*0.055*	*0.055*	*11.65*	*0.0033*	0.59	Significant
f×*f*	1	*1.232E-003*	*1.232E-003*	*0.26*	*0.6166*	0.01	
N× *N*	1	*1.151E-004*	*1.151E-004*	*0.024*	*0.8780*	0.00	
d×*d*	1	*1.769E-004*	*1.769E-004*	*0.037*	*0.8490*	0.00	
Error	17	0.081	4.737E-003				
Total	26	1.85					
SD= 0.069 Mean 1.42 Coefficient of variation = 4.85% Predicted residual error of sum of squares (PRESS) = 0.18						R^2= 96.65% R^2 adjusted = 93.35% R^2 predicted = 90.14% Adequate precision = 24.004	

Table 7. ANN tested architectures MSE and R-values for training, validation and testing of Fd_1, Fd_2 and Fd_3.

Model	Network Structure		Percentage	Samples	RMSE	R value
Fd_1	3-10-1	Training	80	21	4.47413E-4	9.96034E-1
		Validation	10	3	5.73370E-3	9.00364E-1
		Testing	10	3	5.26047E-3	9.62397E-1
Fd_2	3-11-1	Training	75	20	1.39890E-2	9.83323E-1
		Validation	10	3	3.58284E-2	9.39395E-1
		Testing	15	4	1.46822E-1	8.68254E-1
Fd_3	3-11-1	Training	75	21	2.92196E-3	9.82227E-1
		Validation	10	3	3.42195E-3	9.62655E-1
		Testing	15	3	7.23046E-3	9.99763E-1

Table 8. Mathematical models for different delamination factors *Fd* for drilling of jute fabric /polyester biocomposite obtained with ANN Method.

ANN response	
Fd_1	$-1.6398 \times H_1 + 0.1493 \times H_2 - 1.2052 \times H_3 - 0.7614 \times H_4 - 0.3814 \times H_5 + 1.2643 \times H_6 + 1.4256 \times H_7 + 0.4444 \times H_8 - 0.0256 \times H_9 - 0.4312 \times H_{10} + 0.9798$ $\begin{cases} H_1 = \tanh(0.5 \times (0.0032 \times N - 0.0001 \times f + 0.6634 \times d - 4.4658)) \\ H_2 = \tanh(0.5 \times (-0.0158 \times N - 0.0014 \times f - 0.5497 \times d + 7.6695)) \\ H_3 = \tanh(0.5 \times (-0.0071 \times N + 0.0008 \times f - 0.4698 \times d + 3.2338)) \\ H_4 = \tanh(0.5 \times (-0.0051 \times N - 0.0023 \times f - 0.3416 \times d + 7.7537)) \\ H_5 = \tanh(0.5 \times (-0.0167 \times N + 0.0002 \times f + 0.2674 \times d - 1.3141)) \\ H_6 = \tanh(0.5 \times (-0.0080 \times N - 0.0016 \times f - 0.0799 \times d + 4.7291)) \\ H_7 = \tanh(0.5 \times (0.0066 \times N - 0.0004 \times f + 1.0907 \times d - 7.1045)) \\ H_8 = \tanh(0.5 \times (-0.0006 \times N + 0.0052 \times f - 0.2445 \times d - 2.6163)) \\ H_9 = \tanh(0.5 \times (-0.0174 \times N - 0.0039 \times f + 0.4714 \times d + 2.2667)) \\ H_{10} = \tanh(0.5 \times (0.02066 \times N - 0.0019 \times f + 1.3044 \times d - 10.5202)) \end{cases}$
Fd_2	$0.1856 \times H_1 - 1.3672 \times H_2 + 0.3959 \times H_3 + 3.4304 \times H_4 + 1.4228 \times H_5 - 0.1183 \times H_6 - 1.5498 \times H_7 + 0.5441 \times H_8 + 1.8424 \times H_9 - 3.3793 \times H_{10} - 0.0453 \times H_{11} + 1.8329$ $\begin{cases} H_1 = \tanh(.5 \times (0.0168 \times N + 0.0013 \times f + 1.0404 \times d - 10.0074)) \\ H_2 = \tanh(.5 \times (-0.0015 \times N - 0.0030 \times f + 0.8445 \times d - 1.8146)) \\ H_3 = \tanh(.5 \times (-0.0219 \times N + 0.0020 \times f + 0.5208 \times d - 2.3531)) \\ H_4 = \tanh(.5 \times (0.0060 \times N + 0.0010 \times f + 0.3422 \times d - 2.0797)) \\ H_5 = \tanh(.5 \times (-0.0025 \times N - 0.0047 \times f - 0.7390 \times d + 7.4919)) \\ H_6 = \tanh(.5 \times (0.0334 \times N - 0.0021 \times f + 0.8752 \times d - 8.1817)) \\ H_7 = \tanh(.5 \times (-0.0025 \times N + 0.0010 \times f - 0.2736 \times d + 1.5680)) \\ H_8 = \tanh(.5 \times (0.0025 \times N + 0.0019 \times f - 0.4599 \times d + 2.1186)) \\ H_9 = \tanh(.5 \times (-0.0028 \times N - 0.0023 \times f + 0.2517 \times d + 0.8347)) \\ H_{10} = \tanh(.5 \times (-0.0007 \times N - 0.0009 \times f - 0.0955 \times d + 2.3405)) \\ H_{11} = \tanh(.5 \times (-0.0298 \times N + 0.0005 \times f - 0.2519 \times d + 6.3235)) \end{cases}$
Fd_3	$-0.0294 \times H_1 + 0.4314 \times H_2 - 0.3314 \times H_3 + 0.2097 \times H_4 - 1.1851 \times H_5 - 0.3202 \times H_6 + 0.6172 \times H_7 - 0.8388 \times H_8 + 1.2221 \times H_9 + 0.1085 \times H_{10} + 0.3920 \times H_{11} + 2.5024$ $\begin{cases} H_1 = \tanh(.5 \times (0.0009 \times N - 0.00004 \times f - 0.0116 \times d + 0.0701)) \\ H_2 = \tanh(.5 \times (-0.0006 \times N + 0.00008 \times f + 0.0171 \times d - 0.3091)) \\ H_3 = \tanh(.5 \times (-0.0007 \times N + 0.00001 \times f - 0.0234 \times d + 0.4472)) \\ H_4 = \tanh(.5 \times (0.0009 \times N - 0.00006 \times f + 0.0095 \times d - 0.3226)) \\ H_5 = \tanh(.5 \times (-0.0010 \times N - 0.00011 \times f - 0.0589 \times d + 1.1869)) \\ H_6 = \tanh(.5 \times (-0.0022 \times N + 0.00024 \times f - 0.0029 \times d + 0.2842)) \\ H_7 = \tanh(.5 \times (0.0004 \times N - 0.00003 \times f + 0.0219 \times d - 0.4857)) \\ H_8 = \tanh(.5 \times (-0.0001 \times N - 0.00002 \times f - 0.0446 \times d + 0.8271)) \\ H_9 = \tanh(.5 \times (0.0011 \times N + 0.00007 \times f + 0.0582 \times d - 1.1684)) \\ H_{10} = \tanh(.5 \times (0.0001 \times N - 0.00006 \times f - 0.0010 \times d - 0.0102)) \\ H_{11} = \tanh(.5 \times (0.0009 \times N - 0.00005 \times f + 0.0146 \times d - 0.3994)) \end{cases}$

Table 9. Comparison between RSM and ANN approach for different *Fd*.

	Fd_1			Fd_2			Fd_3		
Order	EXP	RSM	ANN	EXP	RSM	ANN	EXP	RSM	ANN
1	1.12	1.24	1.12	1.12	1.25	1.15	1.02	1.05	1.09
2	1.45	1.46	1.45	1.54	1.67	1.54	1.14	1.17	1.21
3	1.64	1.60	1.68	2.17	2.19	2.17	1.44	1.37	1.39
4	1.18	1.19	1.18	1.25	1.15	1.25	1.08	1.04	1.01
5	1.46	1.39	1.46	1.75	1.52	1.51	1.17	1.16	1.12
6	1.53	1.52	1.66	2.18	1.97	1.86	1.38	1.38	1.35
7	1.13	1.07	1.13	1.38	1.45	1.38	1.01	1.01	1.08
8	1.24	1.25	1.25	1.68	1.73	1.68	1.09	1.15	1.17
9	1.30	1.33	1.31	1.90	2.05	1.90	1.38	1.38	1.35
10	1.66	1.62	1.66	1.90	1.72	1.90	1.28	1.20	1.22
11	1.83	1.81	1.83	2.11	2.07	2.11	1.37	1.31	1.32
12	1.85	1.90	1.85	2.77	2.47	2.47	1.40	1.51	1.51
13	1.72	1.65	1.65	1.59	1.64	1.41	1.11	1.22	1.18
14	1.85	1.82	1.86	1.61	1.94	1.61	1.30	1.35	1.32
15	1.89	1.89	1.81	1.68	2.28	1.78	1.56	1.56	1.53
16	1.59	1.68	1.59	2.10	1.99	2.10	1.29	1.27	1.31
17	1.83	1.82	1.83	2.29	2.19	2.40	1.49	1.40	1.44
18	1.82	1.85	1.81	2.66	2.40	2.49	1.64	1.63	1.64
19	1.33	1.31	1.34	2.35	2.57	2.71	1.38	1.43	1.49
20	1.47	1.44	1.47	2.90	2.80	2.90	1.52	1.55	1.61
21	1.49	1.46	1.54	2.94	3.04	2.94	1.78	1.74	1.77
22	1.43	1.45	1.33	2.68	2.53	2.72	1.54	1.52	1.58
23	1.45	1.56	1.44	2.90	2.70	2.90	1.73	1.64	1.73
24	1.51	1.56	1.51	2.96	2.88	2.96	1.82	1.84	1.90
25	1.73	1.70	1.73	2.88	2.94	2.88	1.68	1.66	1.60
26	1.76	1.79	1.76	2.87	3.02	2.96	1.71	1.80	1.75
27	1.84	1.75	1.85	3.07	3.06	3.07	2.02	2.02	1.97

Table 10. Goals and parameter ranges for optimization of cutting conditions for different *Fd*.

Condition	Goal	Lower limit	Upper limit
Feed rate, *f* (mm/min)	Is in range	50	190
Spindle speed, *N* (rev/min)	Is in range	355	1400
Drill, d (mm)	Is in range	5	10
Fd_1	Minimize	1.011	1.782
Fd_2	Minimize	1.011	1.782
Fd_3	Minimize	1.089	2.029

Table 11. Response optimization for response parameters using RSM for different *Fd*.

Test n°	Machining parameters			Response parameters			Desirability
	f (mm/min)	*N* (rev/min)	*d* (mm)	***Fd₁***	***Fd₂***	***Fd₃***	
1	50.000	1085.886	5.000	1.127	1.232	1.025	0.972
2	50.000	1089.754	5.000	1.127	1.234	1.025	0.972
3	50.000	1081.805	5.000	1.128	1.230	1.025	0.972
4	50.000	1067.066	5.000	1.131	1.223	1.026	0.971
5	50.001	1107.844	5.000	1.124	1.243	1.024	0.971
6	50.000	1116.723	5.000	1.122	1.248	1.024	0.971
7	50.000	1054.089	5.000	1.133	1.217	1.026	0.971
8	50.000	1041.842	5.000	1.135	1.212	1.027	0.971
9	50.001	1133.836	5.000	1.119	1.257	1.023	0.971
10	50.000	1035.703	5.000	1.136	1.209	1.027	0.971

Table 12. Comparing the response optimization techniques RSM, GA and fmincon optimization for different *Fd*.

Machining parameters			Response parameters	
f (mm/min)	*N* (rev/min)	*d* (mm)	*Fd*	Response
RSM optimization				
56.535	1340.801	5.003	1.109	***Fd₁***
50.000	738.491	5.000	1.147	***Fd₂***
50.046	1392.963	5.002	1.011	***Fd₃***
GA optimization				
66.422	857.25	7.201	1.098	***Fd₁***
160.01	1369.21	8.161	1.841	***Fd₂***
50.109	365.12	5.124	1.650	***Fd₃***
fmincon optimization				
50.000	841.118	7.147	1.044	***Fd₁***
50.005	356.02	5.004	1.705	***Fd₂***
50.044	349.92	5.001	1.590	***Fd₃***

Figures

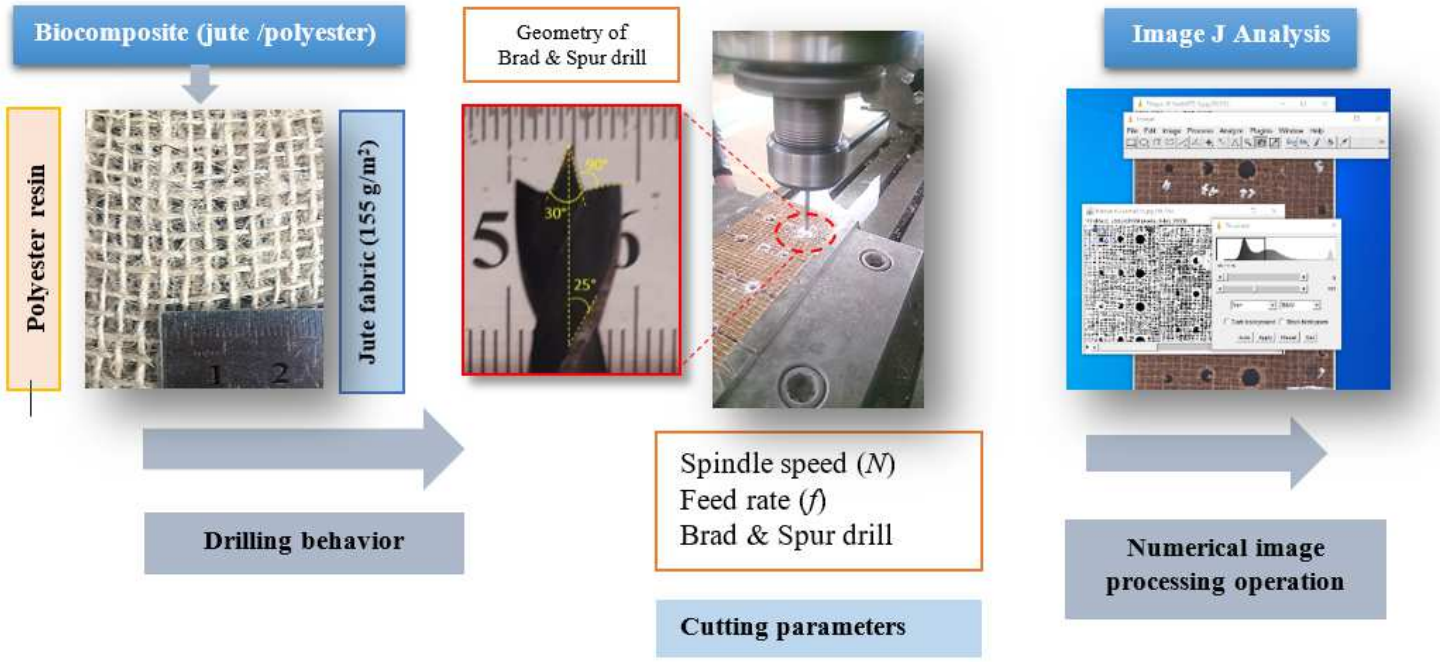

Figure 1

Schematic arrangement of experimental setup.

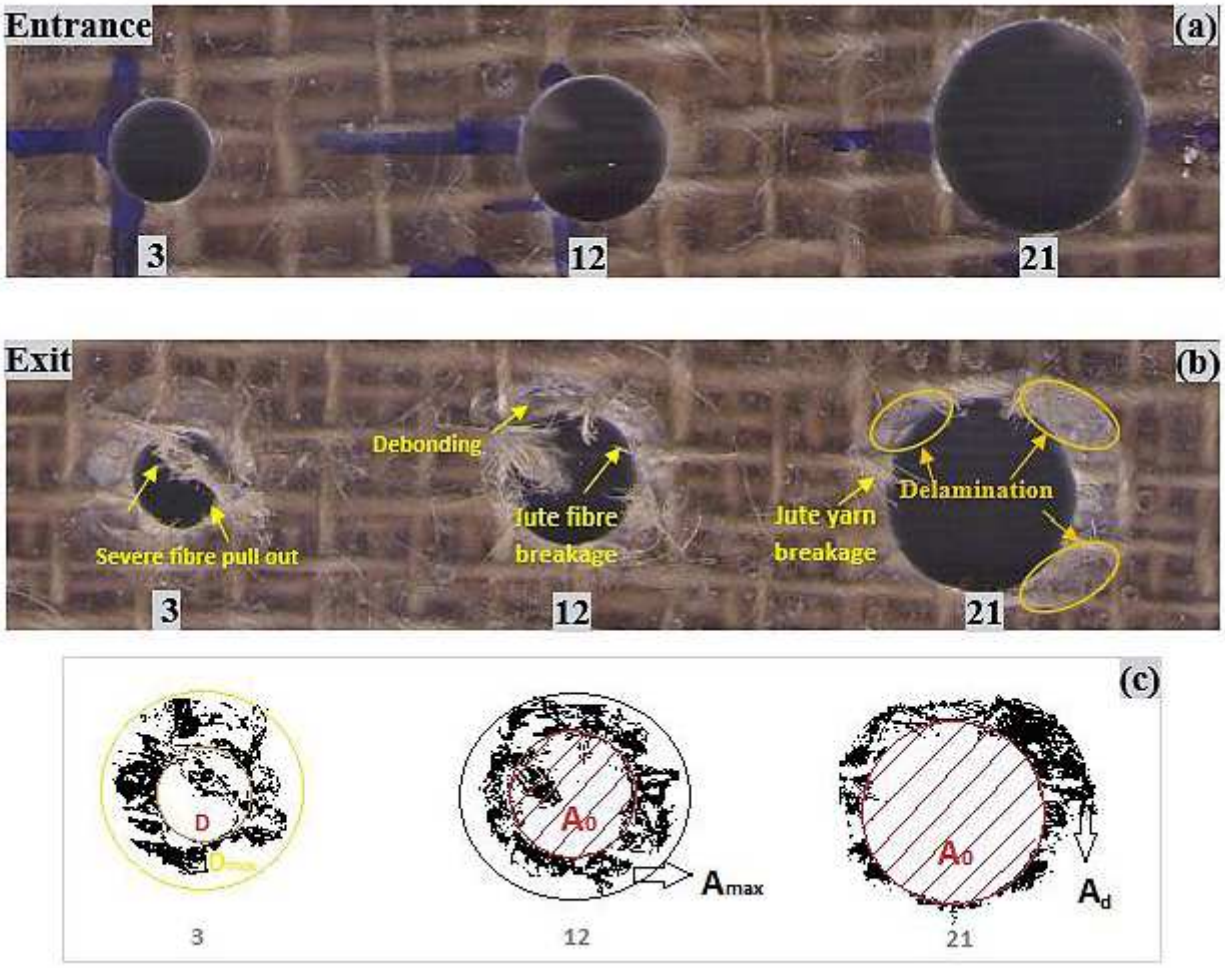

Figure 2

Typical holes drilled on jute fabric/polyester biocomposites for three test (#3, #12 and #21): (a) entrance, (b) exit and typical damage in drilling and (c) determination of different parameters for calculation the delamination factors at the drill and resulting image obtained with ImageJ software.

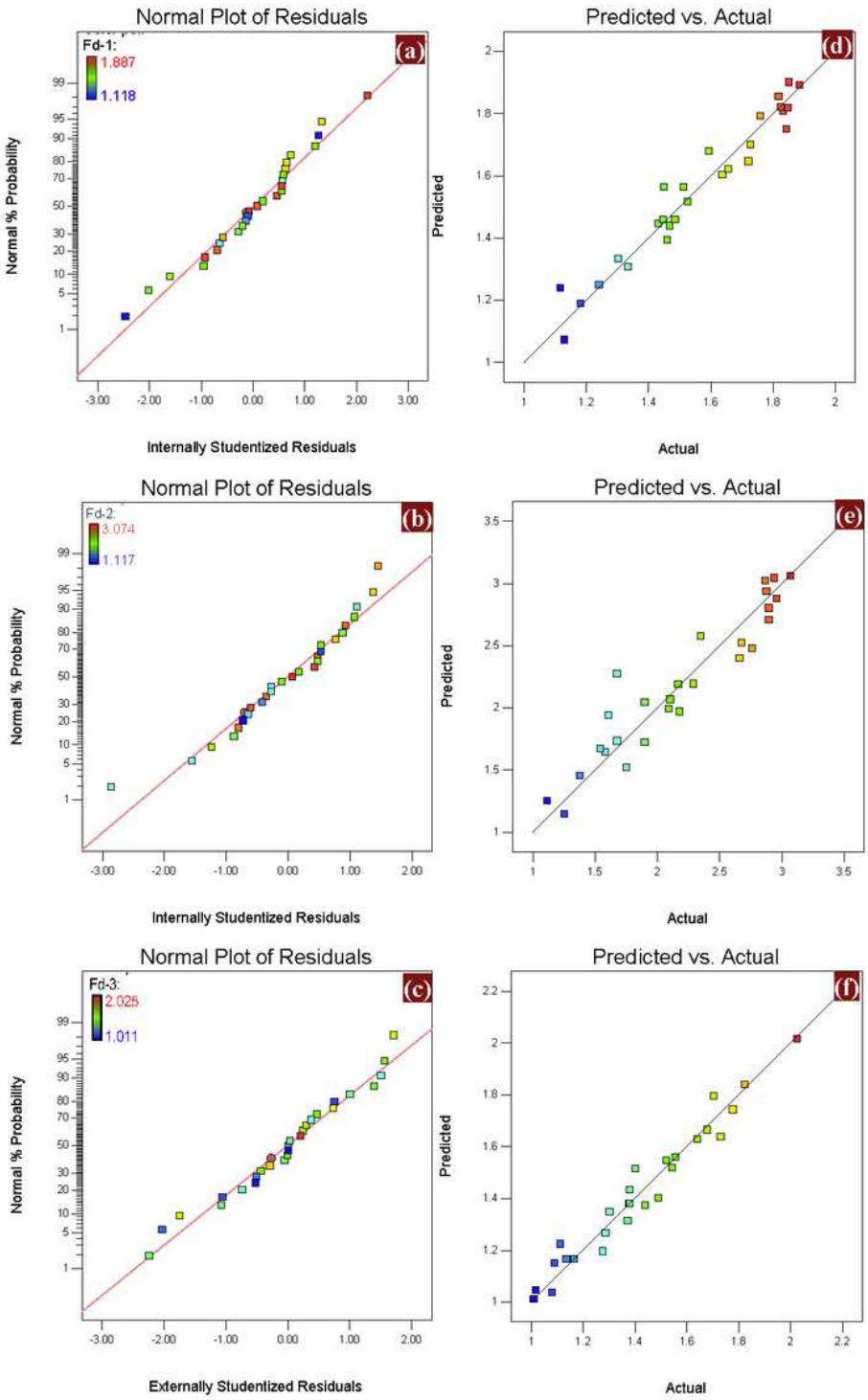

Figure 3

(a–c) Normal probability distribution and (d–f) predicted vs. actual values for different Fd method evaluated.

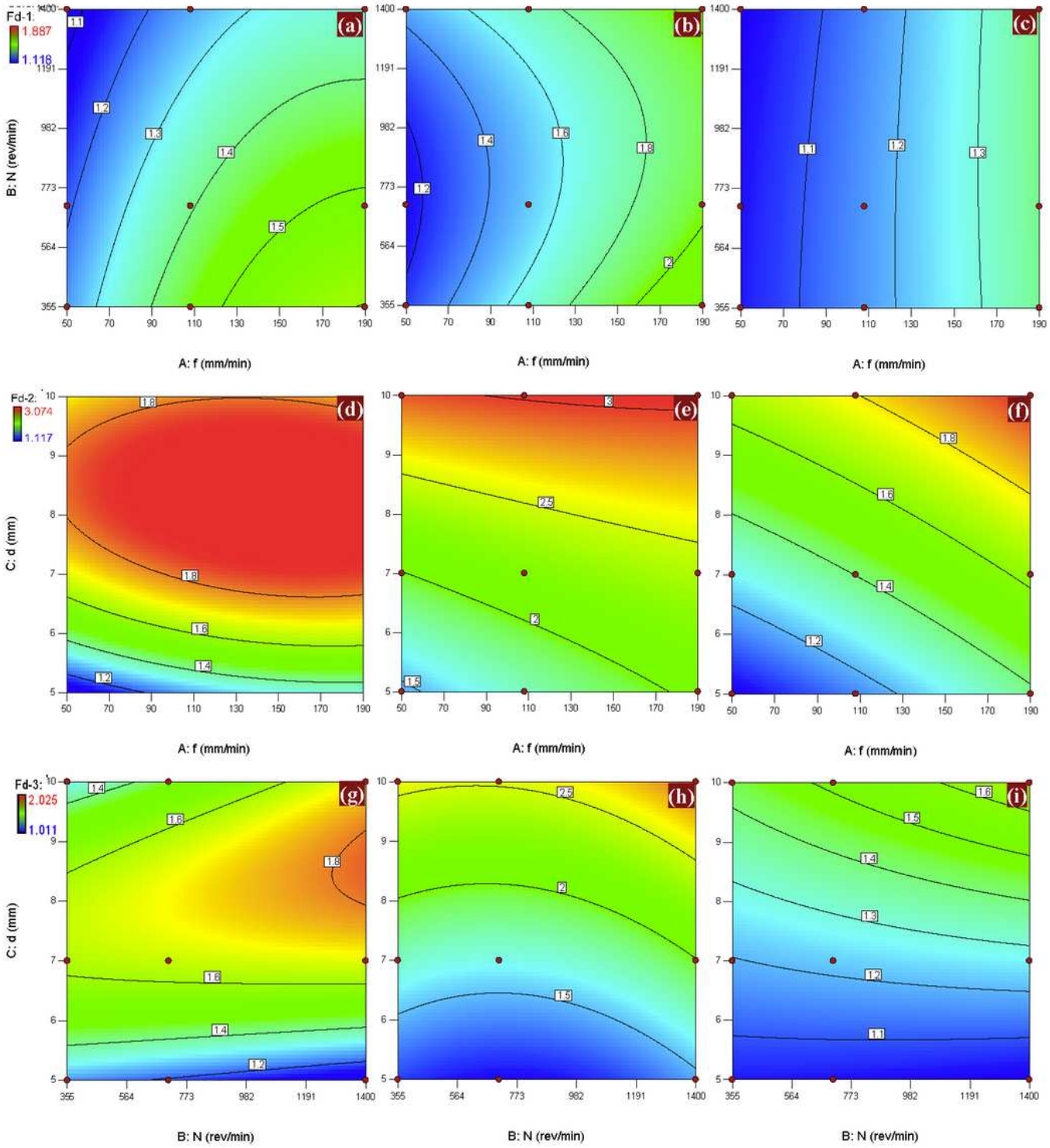

Figure 4

Contour plots for predicted data of the different Fd evaluated as a function of the cutting parameters of the biocomposites produced: (a-c) Fd1 data, (d-f) Fd2 data et (g-i) Fd3 data.

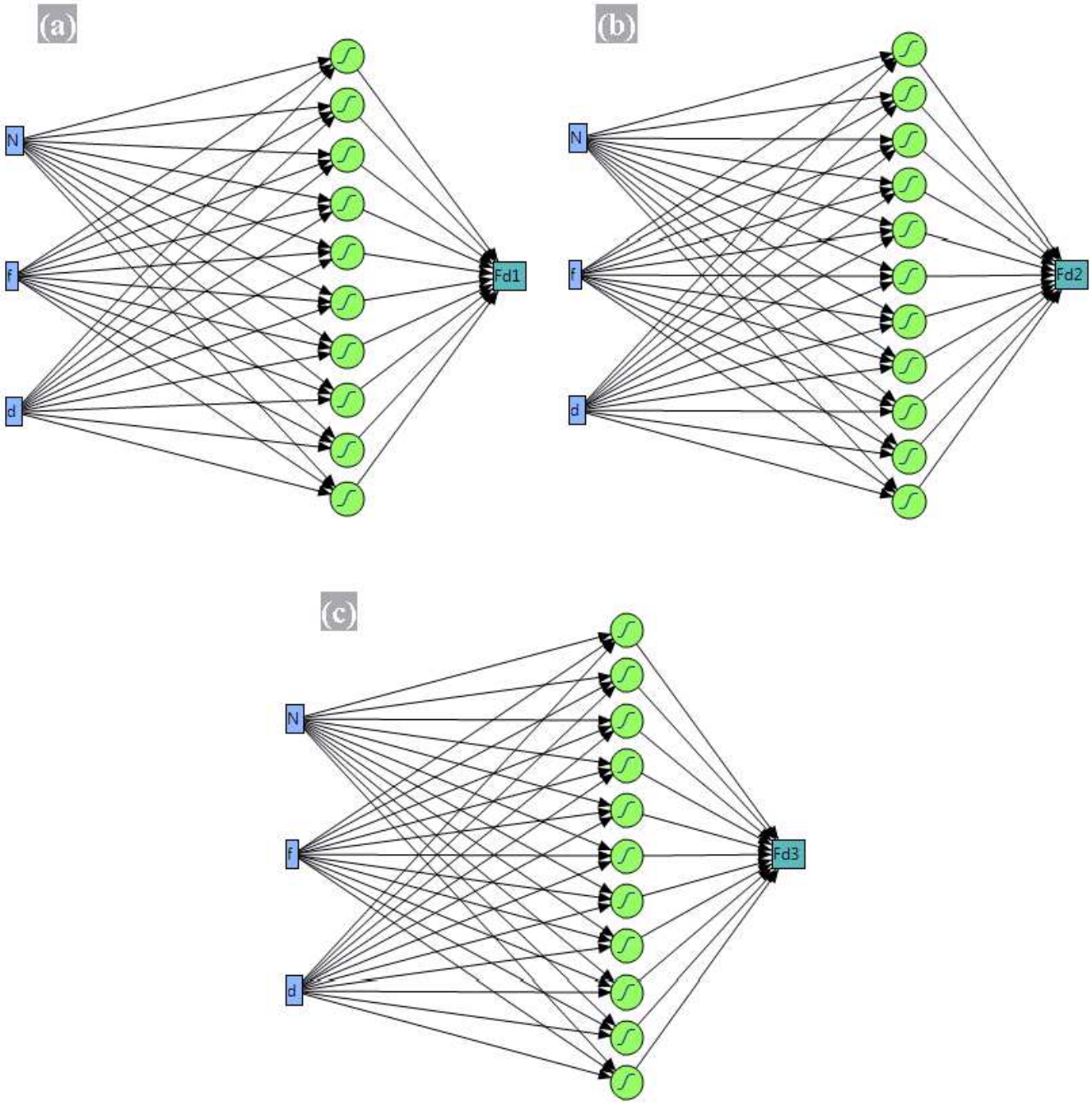

Figure 5

ANN architecture used for (a) Fd1, (b) Fd2 and (b) Fd3.

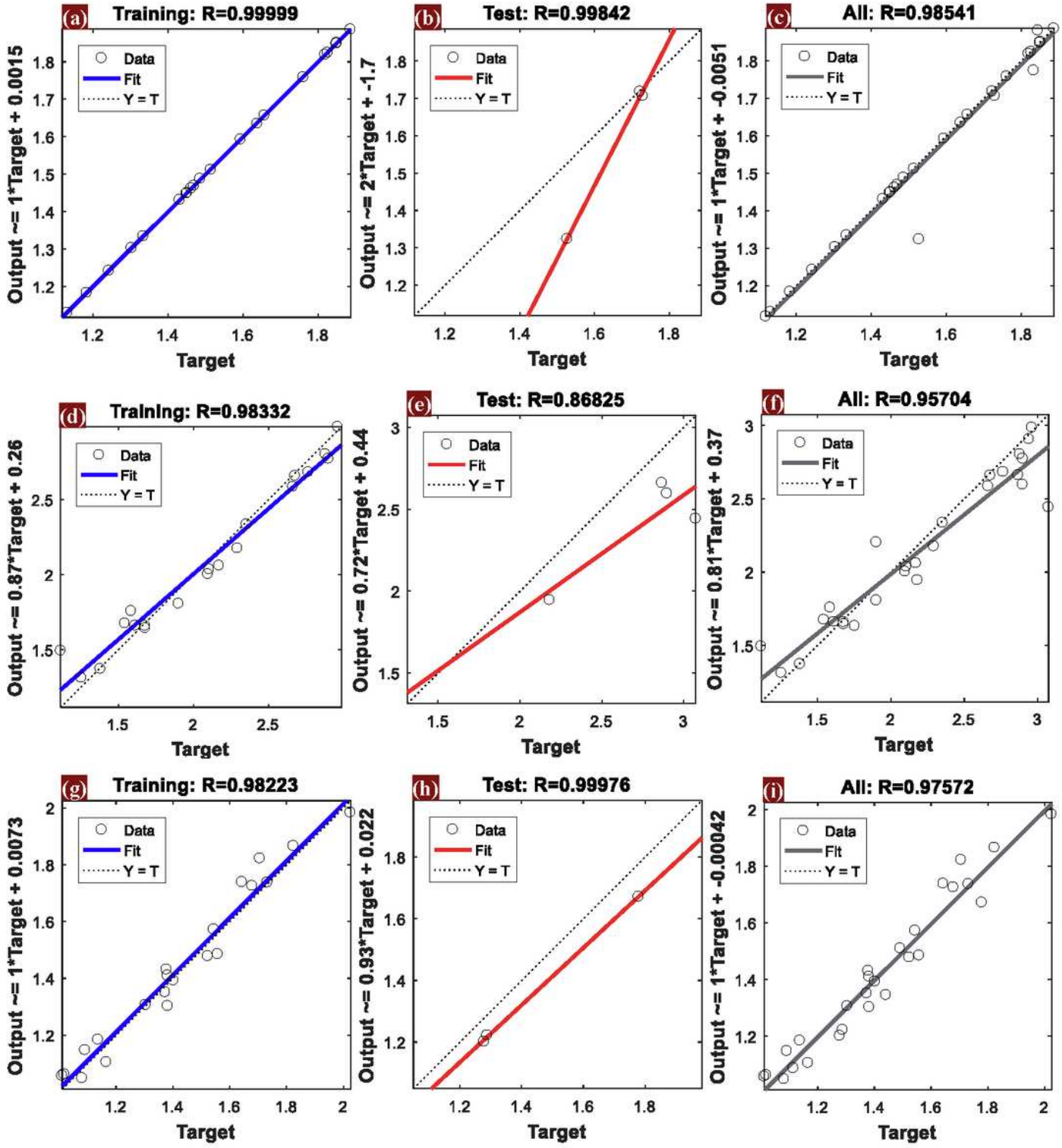

Figure 6

Regression validation scheme of (a-c) Fd1 data, (d-f) Fd2 data et (g-i) Fd3 data.

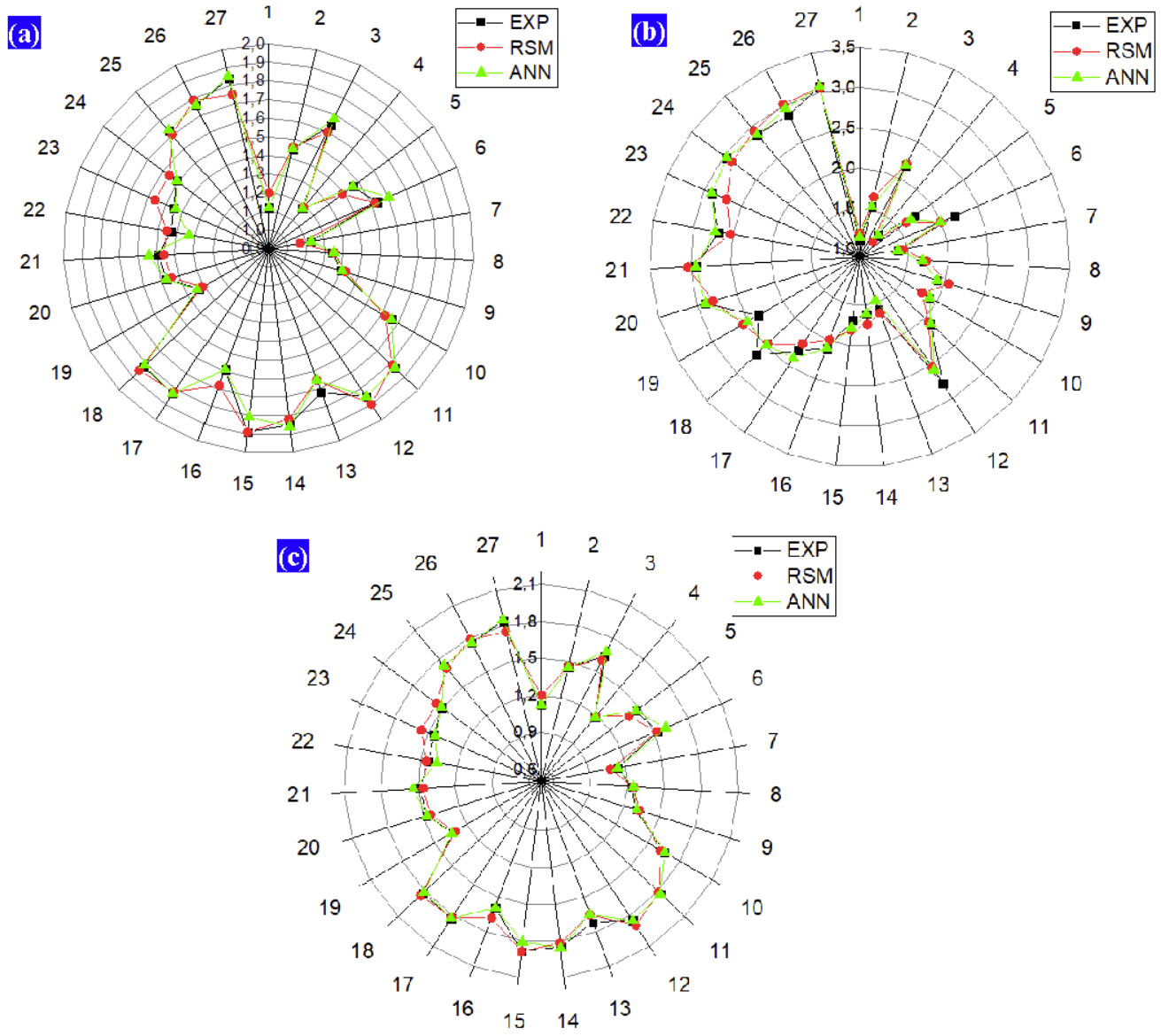

Figure 7

Comparison between experimental and predicted Fd with RSM and ANN models (a) Fd1 data, (b) Fd2 data and (b) Fd3 data.

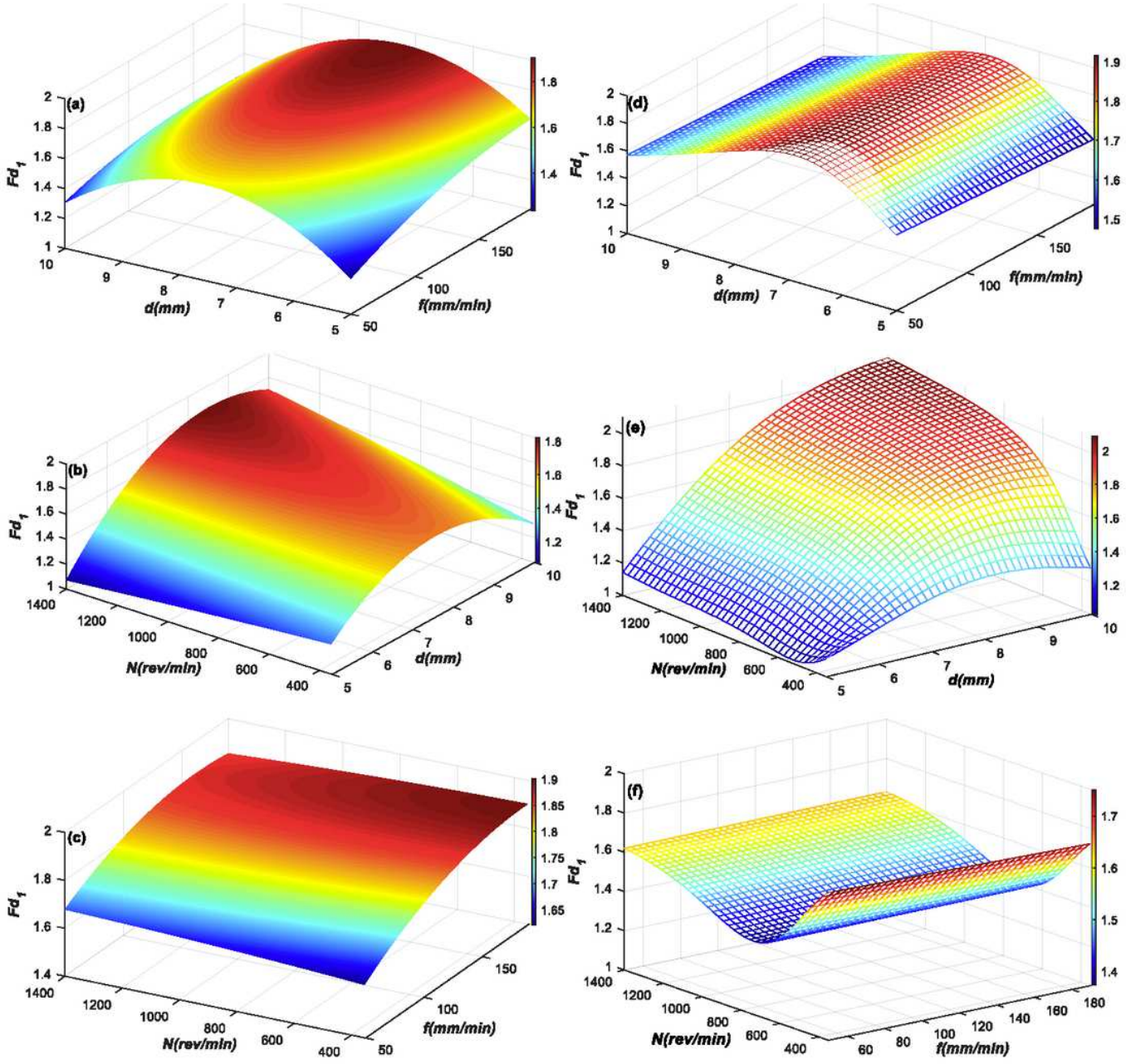

Figure 8

Comparison between 3D surface plots of delamination factor for Fd1 versus f, N and d of biocomposites elaborated (a-c) RSM and (d-f) ANN models.

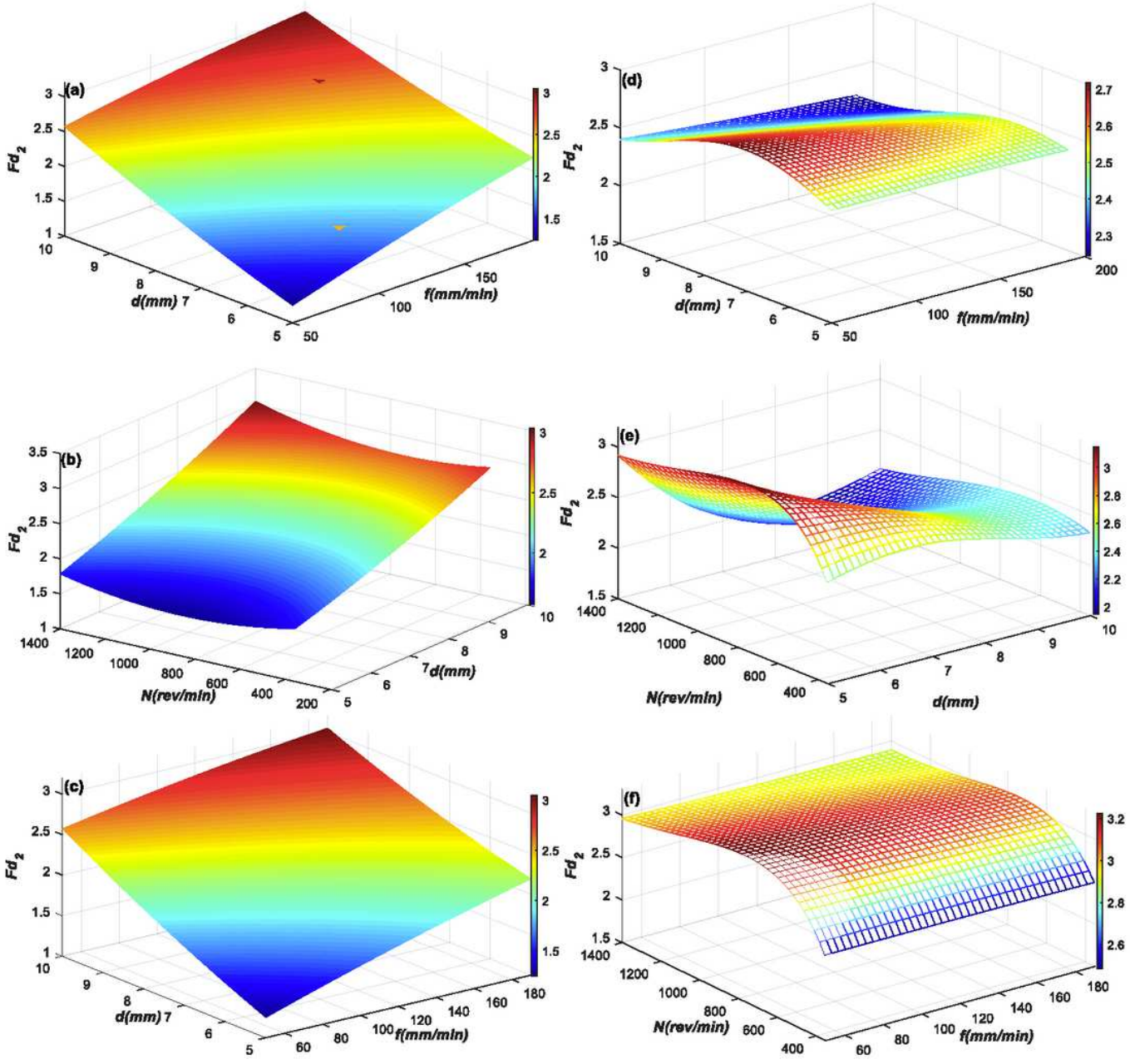

Figure 9

Comparison between 3D surface plots of delamination factor for Fd2 versus f, N and d of biocomposites elaborated (a-c) RSM and (d-f) ANN models.

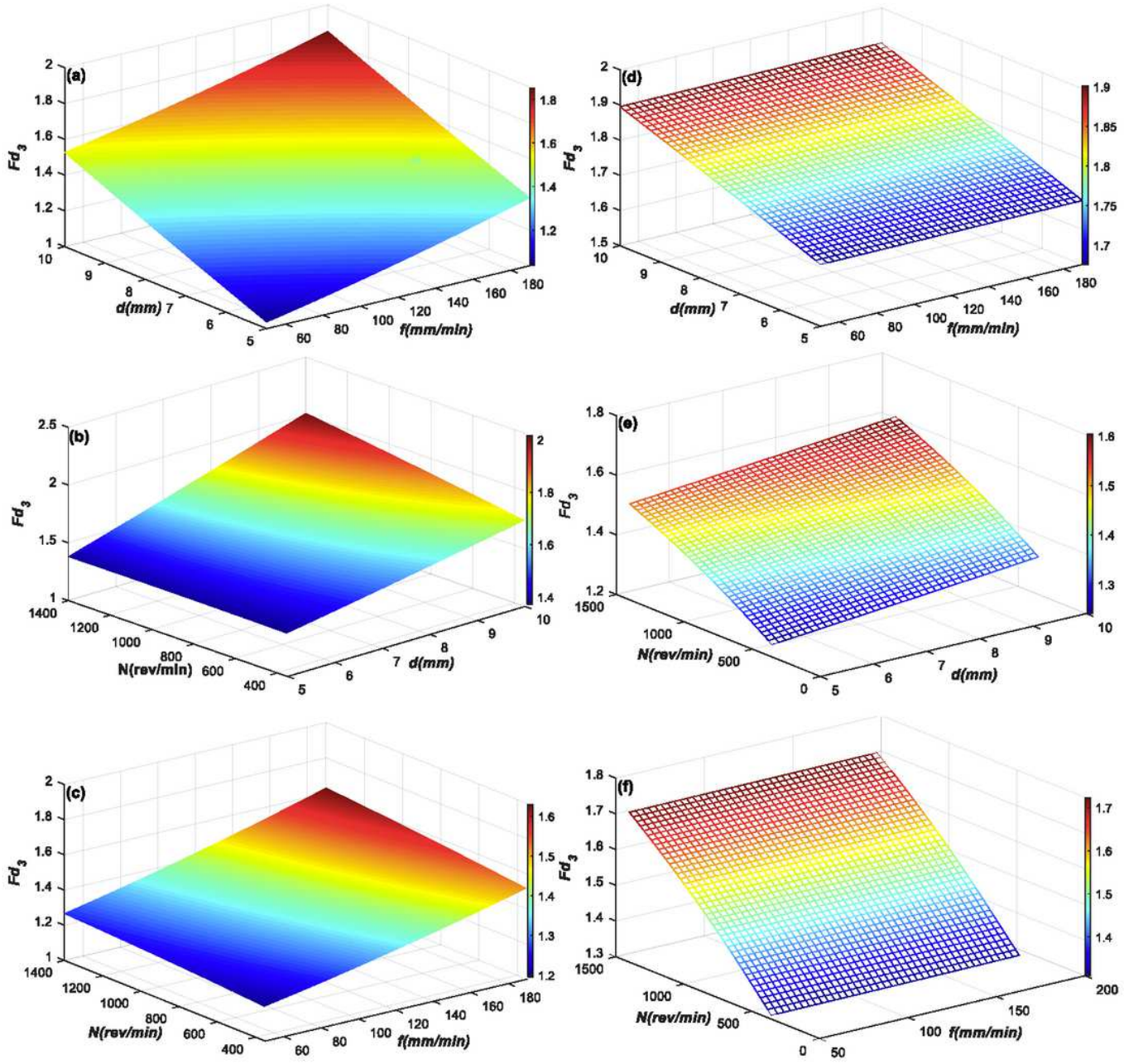

Figure 10

Comparison between 3D surface plots of delamination factor for Fd3 versus f, N and d of biocomposites elaborated (a-c) RSM and (d-f) ANN models.

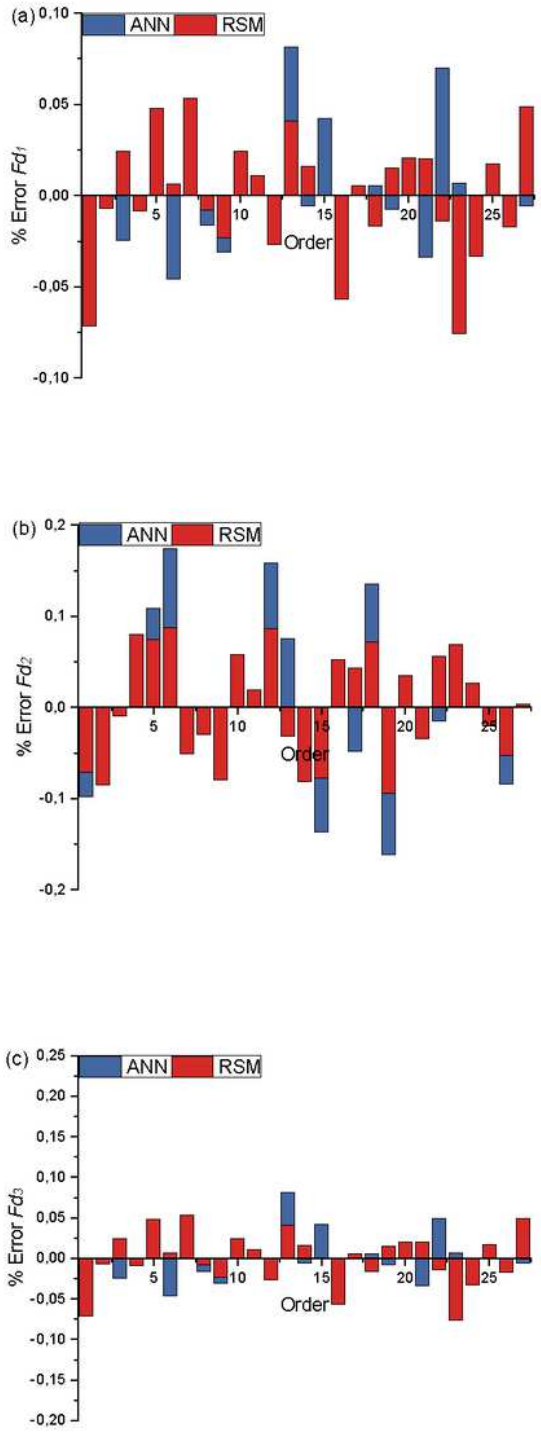

Figure 11

Fd residuals for RSM and ANN (a) Fd1 data, (b) Fd2 data and (b) Fd3 data.

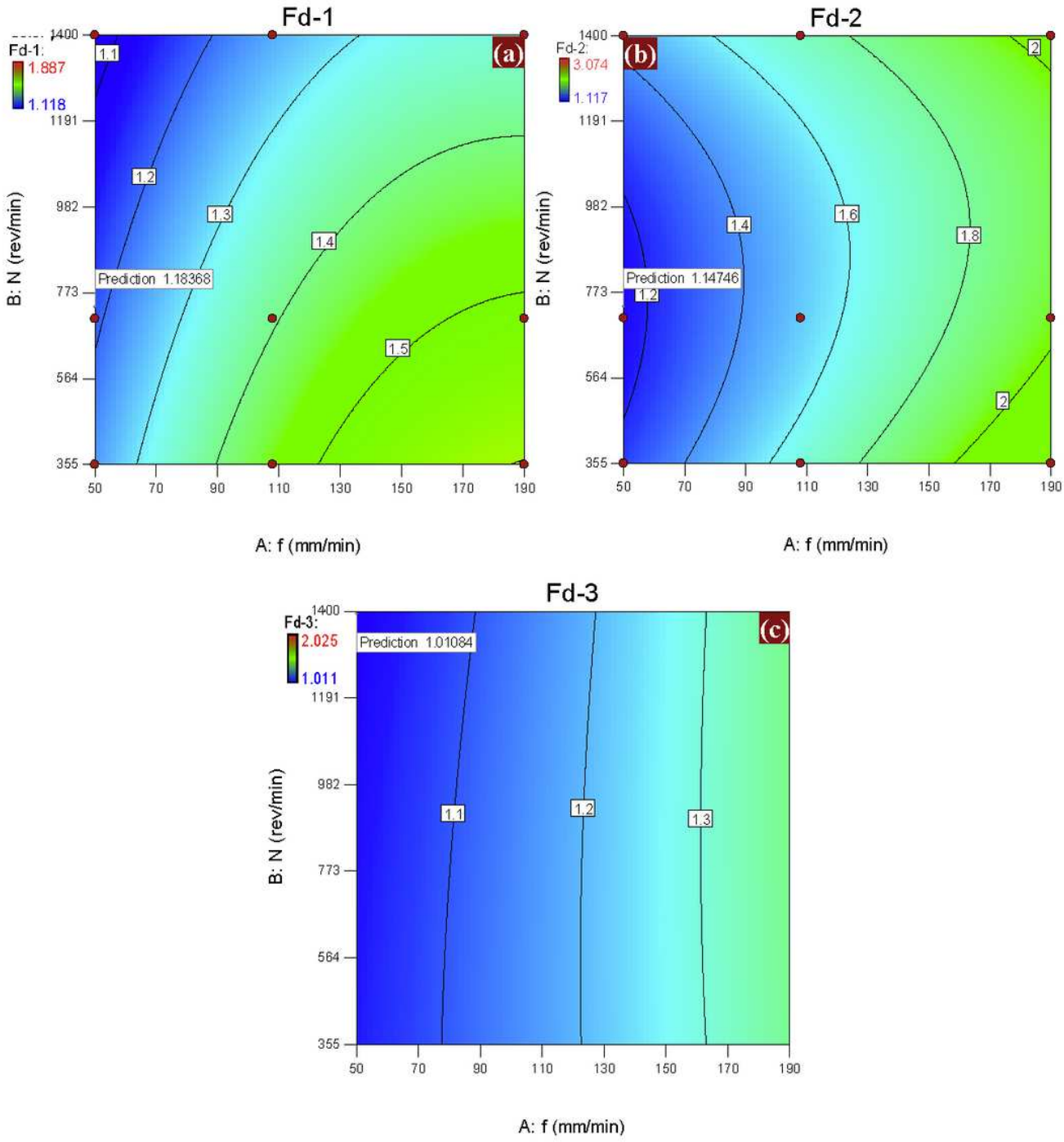

Figure 12

Contour plot of desirability for different Fd method evaluated.

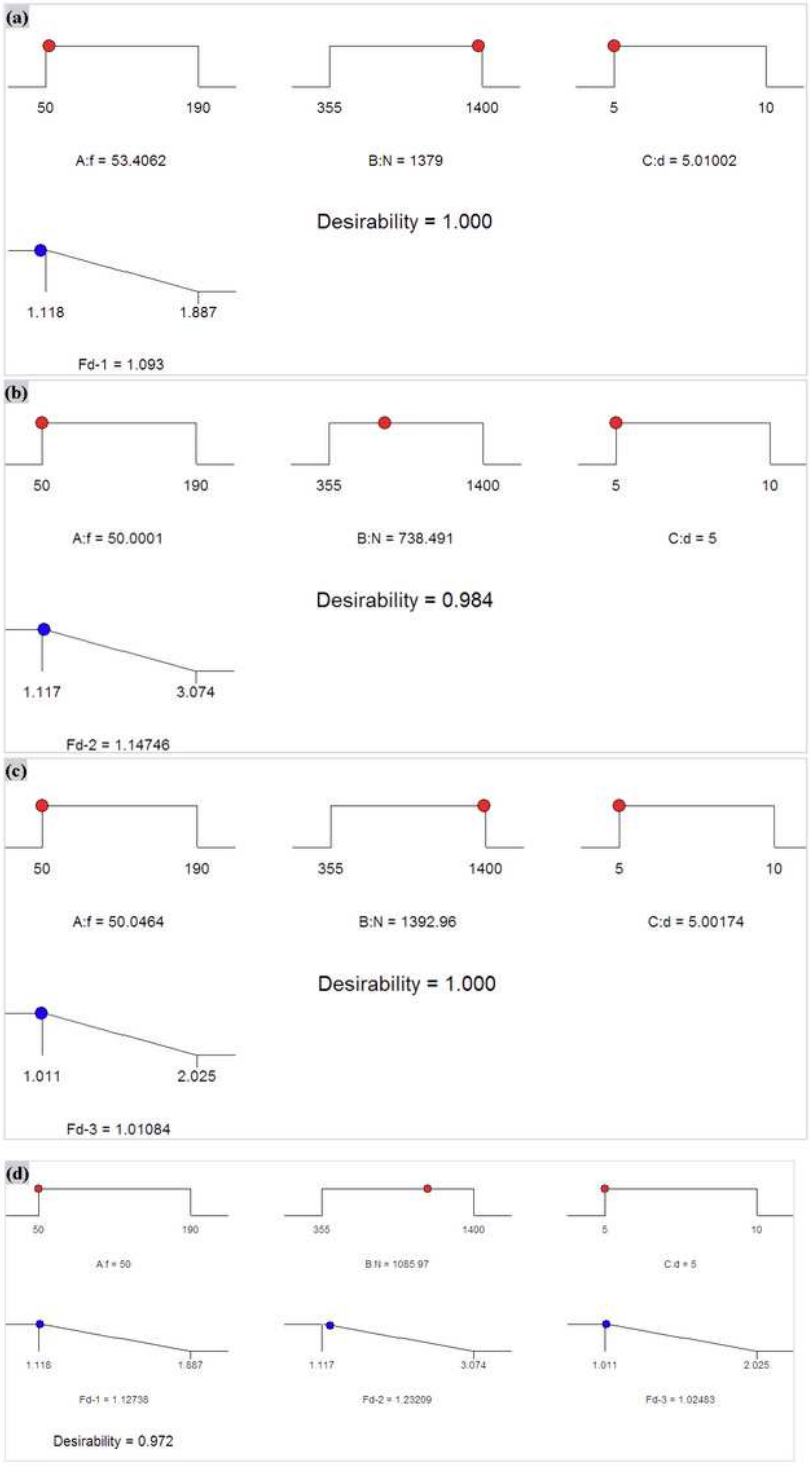

Figure 13

Ramp function graph of multi-objective optimization for different Fd method evaluated (a) Fd1 data, (b) Fd2 data, (c) Fd3 data and (d) Combination data